

# **Ion Current Dependence on Operating Condition and Ethanol Ratio**

**Master's thesis**  
performed in **Vehicular Systems**

by  
**Karin Gustafsson**

Reg nr: LiTH-ISY-EX -- 06/3898 -- SE

December 20, 2006



# **Ion Current Dependence on Operating Condition and Ethanol Ratio**

**Master's thesis**

performed in **Vehicular Systems,**  
**Dept. of Electrical Engineering**  
at **Linköpings universitet**

by **Karin Gustafsson**

Reg nr: LiTH-ISY-EX -- 06/3898 -- SE

Supervisor: **Richard Backman**

GM Powertrain

**Marcus Klein**

Linköpings universitet

**Per Öberg**

Linköpings universitet

Examiner: **Associate Professor Lars Eriksson**

Linköpings universitet

Linköping, December 20, 2006





**Avdelning, Institution**  
Division, Department

Division of Vehicular Systems  
Department of Electrical Engineering  
Linköpings universitet  
SE-58183 Linköping, Sweden

**Datum**  
Date

2006-12-20

**Språk**

Language

Svenska/Swedish

Engelska/English

\_\_\_\_\_

**Rapporttyp**

Report category

Licentiatavhandling

Examensarbete

C-uppsats

D-uppsats

Övrig rapport

\_\_\_\_\_

**ISBN**

\_\_\_\_\_

**ISRN**

LiTH-ISY-EX -- 06/3898 -- SE

**Serietitel och serienummer**

Title of series, numbering

**ISSN**

\_\_\_\_\_

**URL för elektronisk version**

<http://www.vehicular.isy.liu.se>

<http://ep.liu.se>

**Titel**

Title

Jonströmmens beroende av arbetspunkt och etanolhalt

Ion Current Dependence on Operating Condition and Ethanol Ratio

**Författare**

Author

Karin Gustafsson

**Sammanfattning**

Abstract

This masters thesis investigates the possibility to estimate the ethanol content in the fuel using ion currents. Flexible fuel cars can be run on gasoline-ethanol blends with an ethanol content from 0 to 85 percentage. It is important for the engine control system to have information about the fuel. In todays cars the measurements of the fuel blend are done by a sensor. If it is possible to do this with ion currents this can be used to detect if the sensor is broken, and then estimate the ethanol content until the sensor gets fixed. The benefit of using ion currents is that the signal is measured directly from the spark plug and therefore no extra hardware is needed.

To be able to see how the ethanol ratio affects the ion currents, the dependencies of the operating point have been investigated. This has been done by a literature review and by measurements in a Saab 9-3. Engine speed, load, ignition timing,  $\lambda$  and spark plugs effects on the ion currents are especially studied. A black box model for the ion currents dependence on operating point is developed. This model describes the engine speed, load and ignition timing dependencies well, but it can not be used to estimate the ethanol ratio.

**Nyckelord**

Keywords

SI engine, black box modeling, engine speed, engine load, ignition timing



## Abstract

This masters thesis investigates the possibility to estimate the ethanol content in the fuel using ion currents. Flexible fuel cars can be run on gasoline-ethanol blends with an ethanol content from 0 to 85 percentage. It is important for the engine control system to have information about the fuel. In todays cars the measurements of the fuel blend are done by a sensor. If it is possible to do this with ion currents this can be used to detect if the sensor is broken, and then estimate the ethanol content until the sensor gets fixed. The benefit of using ion currents is that the signal is measured directly from the spark plug and therefore no extra hardware is needed.

To be able to see how the ethanol ratio affects the ion currents, the dependencies of the operating point have been investigated. This has been done by a literature review and by measurements in a Saab 9-3. Engine speed, load, ignition timing,  $\lambda$  and spark plugs effects on the ion currents are especially studied. A black box model for the ion currents dependence on operating point is developed. This model describes the engine speed, load and ignition timing dependencies well, but it can not be used to estimate the ethanol ratio.

**Keywords:** SI engine, black box modeling, engine speed, engine load, ignition timing

# Preface

This master thesis has been performed at Vehicular Systems at Linköpings universitet and at GM Powertrain in Södertälje during summer and fall of 2006.

## Thesis outline

This thesis consists of 8 chapters.

- Chapter 1** Background and objectives of the thesis.
- Chapter 2** An introduction to ion currents.
- Chapter 3** A literature review about what ion currents can be used for.
- Chapter 4** Description of the measurements.
- Chapter 5** Description of the preprocessing of the data.
- Chapter 6** Presentation of the qualitative results.
- Chapter 7** Presentation of the quantitative results.
- Chapter 8** Conclusions of the thesis and topics for further work.

## Acknowledgment

I would like to thank my supervisor Richard Backman at GM Powertrain for given me the opportunity to do this thesis. I also want to thank my supervisors in Linköping, Marcus Klein and Per Öberg, for all their help and my examiner, Lars Eriksson, for your interest in my work. Thanks everyone at GM Powertrain in Södertälje, for your assistance with my measurements. I would also thank everyone at Vehicular systems in Linköping for a fun time. Finally I would like to thank Joakim for your support.

# Contents

<b>Abstract</b>	<b>v</b>
<b>Preface and Acknowledgment</b>	<b>vi</b>
<b>1 Introduction</b>	<b>1</b>
1.1 Background . . . . .	1
1.2 Objectives . . . . .	2
1.3 Combustion . . . . .	2
1.4 Ethanol Compared to Gasoline . . . . .	4
<b>2 Ion Currents</b>	<b>6</b>
2.1 Ion Producing Processes . . . . .	6
2.2 Phases . . . . .	9
2.3 Parameters Affecting Ion Currents . . . . .	10
2.3.1 Speed and Load . . . . .	10
2.3.2 Ignition Timing . . . . .	10
2.3.3 Air to Fuel Ratio . . . . .	10
2.3.4 Electrode Gap Size . . . . .	11
2.3.5 Other Disturbances . . . . .	12
<b>3 Uses of the Ion Currents and Previous Related Work</b>	<b>13</b>
3.1 Misfire . . . . .	13
3.2 Knock . . . . .	14
3.3 Information About the Fuel . . . . .	14
3.4 Startup Synchronization . . . . .	16
3.5 Feedback for Ignition Timing . . . . .	16
3.6 Determining the Local Air to Fuel Ratio . . . . .	16
3.7 In HCCI Engines . . . . .	17
<b>4 Measurements</b>	<b>18</b>
4.1 Ethanol Content . . . . .	18
4.2 Measurement Points . . . . .	18
4.3 Spark Plugs . . . . .	19

<b>5</b>	<b>Preprocessing</b>	<b>20</b>
5.1	Normalization . . . . .	20
5.2	Synchronizing . . . . .	20
5.3	Filtering . . . . .	22
<b>6</b>	<b>Qualitative Results</b>	<b>24</b>
6.1	Electrode Gap Size . . . . .	24
6.2	Comparison of Ignitions . . . . .	24
6.3	Air to Fuel Ratio . . . . .	27
6.4	Ethanol Content . . . . .	28
<b>7</b>	<b>Quantitative Results</b>	<b>30</b>
7.1	Modeling . . . . .	30
7.1.1	The Gaussian Model . . . . .	30
7.1.2	Black Box Model . . . . .	34
7.2	Evaluation . . . . .	34
7.2.1	Speed Dependencies . . . . .	35
7.2.2	Load Dependence . . . . .	35
7.2.3	Ignition Dependencies . . . . .	40
7.2.4	Ethanol Dependencies . . . . .	40
<b>8</b>	<b>Conclusions and Future Work</b>	<b>48</b>
8.1	Fulfilled Objectives . . . . .	48
8.2	Future Work . . . . .	49
8.2.1	The Analytical Model . . . . .	49
	<b>References</b>	<b>50</b>
<b>A</b>	<b>Abbreviations</b>	<b>52</b>
<b>B</b>	<b>Measurements</b>	<b>53</b>

# Chapter 1

## Introduction

### 1.1 Background

The use of fossil fuels is causing problems to the environment and the global warming is given more and more attention. In addition, many of the oil producing countries are in political unstable regions and the prices of oil are rising. Hence, alternative fuels are more interesting than ever before. One of these is ethanol, commonly known as alcohol. The main benefit of ethanol compared to gasoline is that it is possible to produce ethanol from biomass and thereby it is considered a renewable fuel.

In flexible fuel cars it is possible to blend ethanol in the gasoline from 0 to 85 percentage. This makes it possible to combine the benefits from the two fuels. The driver of a flexible fuel car can vary the blending of the fuels with cost and access.

Ideally the engine should be optimized for the fuel that is used for the moment, but in flexible fuel vehicles this must be a compromise. It is important for the engine control unit (ECU) to know the blending, to optimize the control for the current fuel to for example avoid knock,  $\lambda$ -control and control of cold starts. In todays cars the measurements of the fuel are done by a sensor. If it is possible to do this with ion currents this can be used to detect if the sensor is broken.

The benefit of using ion currents is that they are measured from the spark gap, and since they are already used to detect misfire and knock, no extra hardware is needed. This is an advantage, because extra costs are avoided in automobiles today. The main problem with this approach is that there are several other parameters that affects the ion currents. Among others, the size of the electrode gap, ignition timing,  $\lambda$ , speed and torque of the engine. The ion currents are also very noisy signals that are hard to interpret.

## 1.2 Objectives

GM Powertrain is interested in knowing if it is possible to estimate the ethanol ratio in the fuel using the ion current signal. The main objective of this thesis is to investigate this. If it is possible an algorithm should be developed, that can be implemented in real time, and does not demand unreasonable much memory or performance of the processor. To make the algorithm robust against different spark plugs, the effect of the electrode gap size on the ion currents is to be investigated. A literature review about ion currents should also be done.

## 1.3 Combustion

This thesis consider a spark ignited (SI) engine. The operation of these is treated in [10]. In this section some basics are summarized.

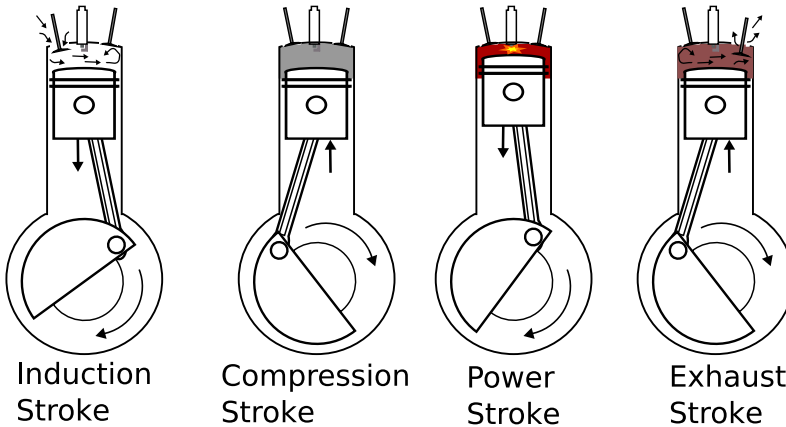


Figure 1.1: The moving of the piston and the gas flows during the four stroke cycle [12].

In an SI engine air and fuel are mixed, and the mixture enters the combustion chamber through an inlet valve. The piston moves down and the mixture fills the chamber. This can be seen in Figure 1.1 as the induction stroke. Somewhere around bottom dead center (BDC) the inlet valve is closed and the compression of the mixture starts, as the piston moves up. This can be seen as the compression stroke in the figure. About 30 degrees before top dead center (TDC), the spark plug ignites the mixture, creating a flame kernel that propagates through the mixture and creates high temperature and pressure and produces a work on the piston when pushing it downwards. This is the power stroke in the figure. After the combustion the exhaust valve is opened and the burned gases are pushed out of the combustion chamber when the

piston is moving down again. This is the exhaust stroke in the figure. Then the inlet valve is opened and the process continues.

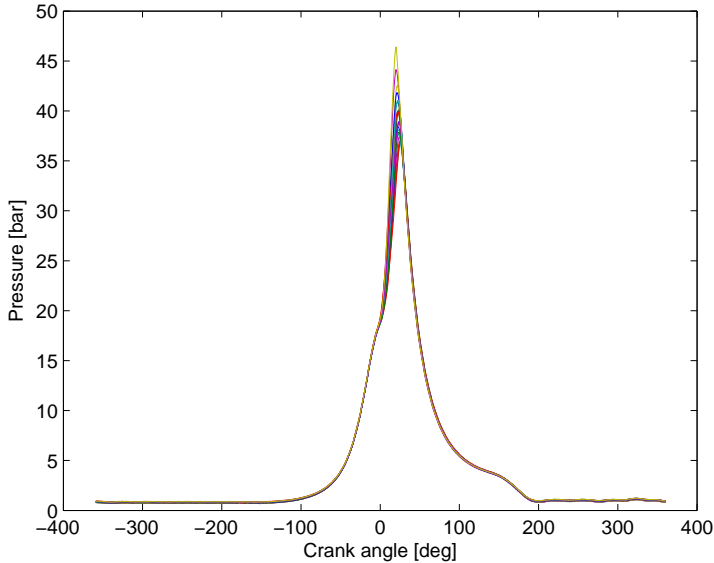


Figure 1.2: The cylinder pressure as a function of crank angle for many different cycles. The pressure rises to a maximum after (TDC), crank angle 0, from the combustion. After the ignition, about 30 degrees before (TDC), differences can be seen in the cycles. These are due to cycle to cycle variations in the combustion process.

In Figure 1.2 the cylinder pressure as function of crank angle degree (CAD) is shown. The figure shows many cycles, to illustrate the differences between them. The pressure rises from the combustion to a maximum about 15 degrees after TDC. Just after the ignition the different cycles have different pressures, although the operating point of the engine is the same. This is called cycle to cycle variations and is a result of that the combustion is not exactly the same every time. The amount of fuel, air and residual gases varies and because of the turbulence in the combustion chamber the same mixture is not obtained every time. The turbulence around the spark plug affects the flame propagation and thus the pressure. These cycle to cycle variations will affect the ion currents. This is one of the reasons that makes the ion currents hard to interpret. During both the flame propagation and the pressure peak ions are created, more about this in Section 2.1.

## 1.4 Ethanol Compared to Gasoline

Ethanol is considered to be a renewable fuel that is quite similar to gasoline, it is liquid and can be fueled in the same way. To be able to run an engine on ethanol some minor changes to a gasoline engine are needed, extra sensors and changes in the ECU. Since ethanol contains water there are also corrosion problems, and therefore some parts in a regular engine have to be changed [7].

There are also some major differences between ethanol and gasoline. Ethanol has a lower heating value. This means that it is not possible to get as much energy out of one kg of ethanol as of one kg of gasoline, and therefore the fuel consumption becomes higher. Ethanol also have a higher research octane number (RON) than gasoline. The higher octane number means that ethanol does not have the same tendency to knock. The knock phenomena is further explained in Section 3.2.

Emissions from an ethanol fueled vehicle contain less carbon monoxide, carbon dioxide and hydrocarbons, but since ethanol has lower vapor pressure there are problems with the cold starts performance. The Reid vapor pressure (RVP) of ethanol are 42.7 kPa, compared to 60 kPa for gasoline. The RVP for ethanol-gasoline blends have a maximum at 10% ethanol and decreases for both higher and lower blends. Gasoline consists of many different hydrocarbons, some of which are very volatile. This makes the RVP higher than the one of ethanol that only consists of one chemical compound. Since some of the fuel have to be vaporized in order to start the combustion this is a problem. Especially in colder climates. In E85 there are 15% of gasoline added to the ethanol to improve the cold start ability. This reduces the problem but it does not eliminate it [7]. In Sweden, the gasoline content are increased in the winter to 21% [1].

There exist some other differences between the fuels. In [6] it is stated that ethanol has a lower combustion temperature than gasoline. The initial combustion rate is faster for ethanol than for gasoline, and ethanol has a shorter combustion duration [20]. Table 1.1 summarizes some of the fuel parameters that are different for ethanol and gasoline. For comparison the table also includes methanol and iso-octane.

<b>Fuel</b>	<b><math>H_{low}</math> [MJ/kg]</b>	<b>RON</b>	<b>C/H</b>	<b><math>(A/F)_s</math></b>
Gasoline	44	95	0.53	14.7
Ethanol	26.9	107	0.33	9.8
Iso-octane	44.3	100	0.44	15.1
Methanol	20	106	0.25	6.5

Table 1.1: Major fuel parameters of some fuels.  $H_{low}$  is the energy content in a kg of the fuel. RON is how high the tendency is to not knock. Fuels with higher values does not knock that easily. Iso-octane is the reference fuel when comparing octane number and therefore has the value 100. C/H ratio is the ratio between carbon and hydrogen. This can affect the conductivity of the fuel's gases and is therefore interesting for the ion currents.  $(A/F)_s$  is the stoichiometric air to fuel ratio, more about this in Section 2.3.3.

# Chapter 2

## Ion Currents

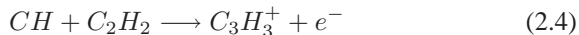
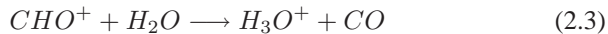
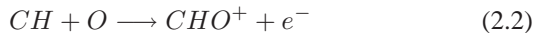
The idea behind the ion current is that when the flame kernel propagates and when the pressure and temperature rise from the combustion, the gases in the cylinder create ions. Ions are created both of chemical reactions in the flame front and of thermal ionization after the flame front. How much ions that are created depends on the combustion, and therefore it is possible to get information direct from the combustion chamber from each cylinder individually by measuring the ion current. This without having to add any extra sensors if the spark plug is used as a sensor. But since the signal is noisy and rather complex, it is hard to interpret. Today the ion current signal is used for startup synchronization and to detect misfire and knock, but many more applications have been considered, see Chapter 3.

### 2.1 Ion Producing Processes

In an ideal combustion the fuel and air react and produce carbon oxide and water. The chemical reaction can be written as (2.1) where iso-octane,  $C_8H_{18}$ , is the fuel.

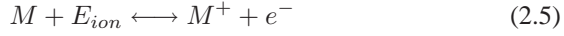


This reaction is the sum of many different reactions, and ions are produced in several steps. Some examples of reactions that include ions are:



These ions and many others are produced in the chemical reactions of the flame. When ions are produced during reactions like (2.4) it is called chemi-ionization or chemical ionization. The other main ionization is thermal ion-

ization. This ionization has only one reactant, and the ions are created because of high temperature and pressure in the gas. (2.5) shows thermal ionization, where  $M$  is an arbitrary specie and  $E_{ion}$  is the ionization energy.



One model of how much ions that are present in the gas is Saha's equation (2.6). The equation describes the degree of ionization of different species, and assumes that the gas is in thermal equilibrium i.e. that the ionization equilibrium is achieved immediately.

$$\frac{n_i n_e}{n_{i-1}} = 2 \left( \frac{2\pi m_e kT}{h^2} \right)^{\frac{3}{2}} \frac{B_i}{B_{i-1}} e^{-\frac{E_{ion}}{kT}} \quad (2.6)$$

where

- $n_i, n_{i-1}$  : number of density of the state  $i$  and  $i - 1$ . This means the number of atoms per volume unit that are in state  $n_i$  and  $n_{i-1}$ .
- $n_e$  : the electron number density
- $k$  : Boltzmann's constant
- $m_e$  : the electron mass
- $T$  : the absolute temperature
- $h$  : Plank's constant
- $E_{ion}$  : the ionization energy of state  $i$
- $B_i$  : the internal partition function

Different species that are present in the combustion will contribute to the thermal ionization in different ways, depending on the ionization energies. The ones with the lowest ionization energy will contribute the most. Table 2.1 shows some of the species and their ionization energy. It has been found that  $NO$  is the dominating contributor to the thermal ionization [15].

<b>Species</b>	<b>Ionization energy [eV]</b>
$N_2$	15.5
$N$	14.53
$O_2$	12.2
$O$	13.614
$H_2$	15.427
$H$	13.595
$H_2O$	12.6
$OH$	13.18
$CO$	14.05
$CO_2$	13.84
$NO$	9.25
$C_2$	12.0
$CH$	11.13
$CH_2$	11.82 & 10.4
$CH_3$	9.84
$CH_4$	12.61
$C_2H_2$	11.41
$C_3H_3$	8.67
$CHO$	9.88
$CH_3O$	9.2
$Na$	5.138
$K$	4.339

Table 2.1: Ionization energy of some species, Table 6.1 in [15] on page 47. The ionization energy is a measure of the energy needed to ionize a molecule. During the combustion the pressure and temperature rise and the species with the lowest ionization energy will be ionized first. The first part of this table shows species that are common in the combustion and the last two are alkali metals, that because of their very low ionization energy contribute much to the ion current if they are present in the combustion.

## 2.2 Phases

The ion current has three phases. These are shown in Figure 2.1.

- **The ignition phase**  
In this part the main contributor is the ignition process.
- **The flame front phase**  
The ions that are created in the flame front is the main contributor in this part of the signal. The peak of the signal occurs when the flame is in contact with the spark plug electrodes [2]. The dominant process for this part is chemi-ionization.
- **The post flame phase**  
High pressure and temperature of the combustion produces ions in this part of the signal. The dominant process for this part is thermal ionization. The position of the peak in this part of the signal is strongly dependent on the position of the peak of the cylinder pressure.

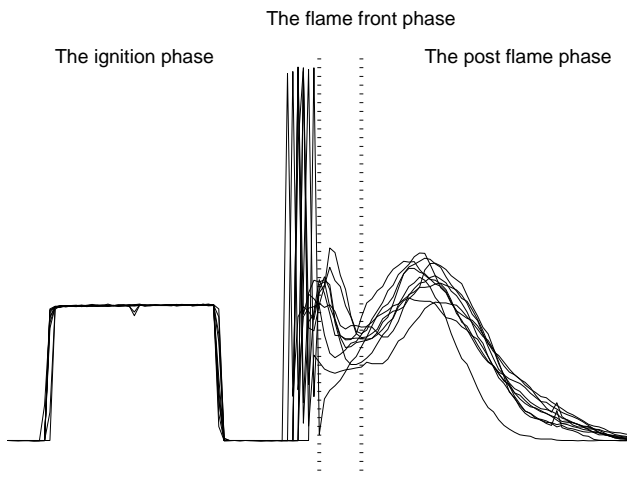


Figure 2.1: The three phases of the ion currents showed for several cycles. The flame front phase and the post flame phase give information about the combustion.

In the rest of the thesis the flame front peak will be called the first peak and the post flame peak will be called the second peak. This notation will be used despite the fact that the two peaks sometimes are divided into several peaks, and that the phases can be hard to separate.

## 2.3 Parameters Affecting Ion Currents

The combustion process is dependent of several parameters and the most important, except for the fuel, are listed in this section.

### 2.3.1 Speed and Load

The amplitude of the signal is affected by the engine speed and the engine load, and of other parameters that are harder to measure. The absolute level of the peaks are therefore not a good measurement [5]. With very light loads the ion current curve becomes flatter until there is no longer a maximum [13]. In [16] an experimental study on load and speed dependence was done. There it was found that the first peak was not affected by different loads. The amplitude of the second peak shows a clear dependence on the load and increases with increased load. Since the second peak is related to the cylinder pressure this is not unexpected.

### 2.3.2 Ignition Timing

How many degrees before TDC the mixture is ignited, affects the combustion. If the ignition is too early the pressure in the combustion chamber rises too early before TDC, and then the rising pressure works against the piston movement and brakes the piston instead of accelerates it. The top pressure at the peak also becomes much higher since the pressure rises from the combustion when the volume of the cylinder is small. Too early ignition results in less work produced.

If the mixture is ignited too late, it results in a lower pressure peak and that the pressure peak comes later in the cycle. This also results in less work produced. The optimal ignition angle is defined as when the most work are produced. When there is a risk for knocking the ignition is moved away from the optimal to avoid too high pressures. Since the ignition timing affects the cylinder pressure shape it also affects the shape of the ion currents.

### 2.3.3 Air to Fuel Ratio

Another parameter that affects the ion currents is  $\lambda$  or normalized air to fuel ratio.  $\lambda$  can be calculated as:

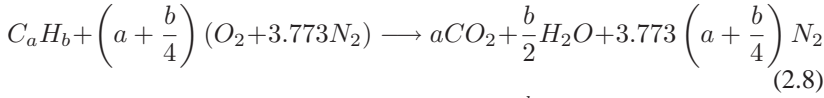
$$\lambda = \frac{m_a}{m_f(A/F)_s} \quad (2.7)$$

A stoichiometric combustion reaction between a general hydrocarbon,  $C_aH_b$ , fuel and air produces only water and carbon oxide, see (2.8). The

where

$m_a$	:	Mass of air
$m_f$	:	Mass of fuel
$(A/F)_s$	:	Stoichiometric air to fuel ratio

$(A/F)_s$  can be calculated as (2.9) [10].



$$(A/F)_s = \frac{34.56(4 + \frac{b}{a})}{12.011 + 1.008 \frac{b}{a}} \quad (2.9)$$

In [16] the dependence of the ion currents on  $\lambda$  is studied experimentally and Figure 2.2 shows a  $\lambda$ -scan at 2500 RPM at constant inlet pressure of 101.3 kPa with Iso-octane. The change in the first peak is related to the chemi-ionization in the flame kernel in the vicinity of the spark plug and this is directly affected by  $\lambda$ . The changes that can be seen in the second peak depends on that  $\lambda$  affects the combustion, and thereby the pressure and temperature and thereby also the currents. A maximum of the signal were found at  $\lambda = 0.85$ .

The magnitude of the first peak is found closely related to the air to fuel ratio close to the electrodes [2]. In [13] the dependence on  $\lambda$  is explained. When there are excess air i.e. high  $\lambda$ , the temperature in the combustion chamber becomes lower and the recombination of ions are faster, and the ion current becomes lower. The temperature affects mostly the second peak.

### 2.3.4 Electrode Gap Size

In [11] a cooling effect on the gas from the electrodes is found. The electrodes cool the burned gases and thereby there less ions are produced. When the distance between the electrodes are smaller, the ion current is also smaller because of the cooling. Since temperature is very important for the gas to form ions, this effect is interesting. In this paper a simplified geometry of the electrodes is used instead of a spark plug, but a connection between the first peak, the electrode shape and the gas flow was found. The effect on the gases of the electrodes were investigated by laser induced fluorescence imaging and it was found that less  $NO$  ions are formed in the vicinity of the electrodes. This was an experiment with laminar gas flow, and the effect can be less in turbulent flow. One conclusion of this paper is when the spark gap is decreased, the ion current amplitude also decreases. Another aspect is that a smaller distance would make it easier to get a signal and the signal would be higher.

These two scenarios are conflicting and to try which one that is the dominating effect, different spark gaps were tested during the measurements. More

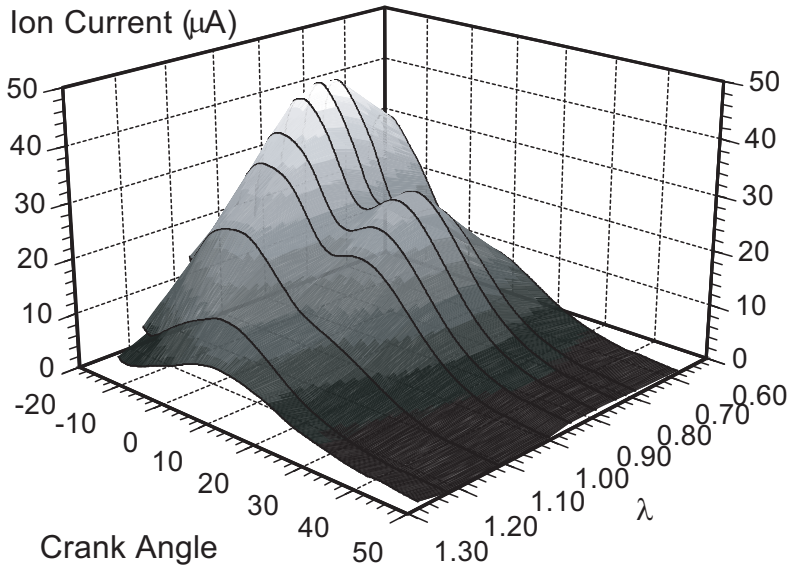


Figure 2.2:  $\lambda$ -scan using averaged ion current signals acquired from the engine at 2500 RPM and a constant inlet manifold pressure, 101.3 kPa with Iso-octane. Figure 4 on page 4 in [16]. Both peaks of the signals depends on  $\lambda$ .

about this in Chapter 4.

### 2.3.5 Other Disturbances

The ion current signal is very rich on information but not yet fully understood. Except for the earlier mentioned parameters also many other unmeasurable disturbances affects it. Examples of those are air humidity and temperature, amount of residual gases, variations in the fuel, engine wear and many others. Therefore conclusions about the ion currents dependence on different parameters such as ethanol content should be drawn with care.

## Chapter 3

# Uses of the Ion Currents and Previous Related Work

Much work has been done in the subject of ion currents. This chapter describes some of the ways the ion currents can be used, both applications that are in production cars today and those who are under development.

### 3.1 Misfire

California on board diagnostics (OBD-2) requires that every misfire should be detected. Misfire means that the gas in the cylinder for some reason is not ignited. This is a severe problem, since as a consequence unburned gasoline reaches the catalytic converter. The unburned gasoline is potentially hazardous for the catalytic converter.

Ion currents can be used to detect misfire since when there is no combustion, there will be no current. A problem with this is thus at very light loads, the ion currents are very small even when there is no misfire. For such conditions, the difference between normal cycles and cycles with misfire is very small [4]. In [4], nine different engines were tested to get a good threshold for deciding when misfires occurred. The suggested criteria is engine dependent and has to be decided in cooperation with the engine designer. To be able to detect misfire accurately the ion currents are filtered, with a 200 Hz low pass filter. The conclusion in [4] about misfire is that using the suggested method, ion currents can be used to get a 100% misfire detection.

In [19] the ion current signal is used to detect misfire and with the use of a special type of spark plug it is possible to reignite the mixture to avoid a total misfire. The projected surface gap spark plug that is used in [19] makes it possible to have a short-duration ignition and therefore gives the ECU a chance to reignite the fuel mixture. When using this technique, no unburned gasoline reaches the catalyst. Another benefit is that the engine runs smoother. In [19]

the ion current is integrated through the cycle to detect misfire, instead of a low pass filter as in [4]. The integrated ion current signal is compared to a threshold to decide whether it has been combustion or misfire.

## 3.2 Knock

Knock is a severe problem for SI engines. Knock means that some parts of the gas self-ignites before it has been reached by the propagating flame kernel. It results in noise and thereby the name. When knock occurs much chemical energy is released fast and a very high local pressure chamber is created. This leads to pressure waves in the combustion chamber. If it is allowed to continue it can damage the engine. Knock can be avoided by decreasing the spark advance. This means that the ignition is moved later, so that the end-gas temperature won't get so high that knock occurs. The best, but most expensive way of detecting knock is to use a pressure sensor. The most common way is to use an extra knocking sensor, but it is also possible to detect knock by ion currents [10].

Knock results in high frequency oscillations in the second peak of the ion current. These oscillations usually has a frequencies over 5 kHz. The intensity of the knock are also possible to see on the ion currents. The benefits of using ion currents are that it is more reliable than a knock sensor and that extra hardware is avoided [4].

In [14] the ion current detection system is compared to the conventional type of vibration detection method and the conclusion is that the conventional type is affected by mechanical noise from the engine, which the ionic system is not. The ionic system also had a higher signal to noise ratio especially at speeds over 6000 RPM. Another benefit of using ion currents is that the individual cylinders could be separated.

## 3.3 Information About the Fuel

Since all the chemical reactions that takes place in the combustion chamber are not completely known, it is hard to model the dependence on different fuels by theoretical models. One paper that discuss how fuels affects on the ion currents is [16] where ion currents from different fuels and additives are studied. Ethanol is among the fuels tested and there are large differences in the amplitudes of the signals from ethanol and from gasoline, see Figure 3.1.

The experiment with alcohols have been done for pure alcohols and not for any alcohol-gasoline blends. The paper describes the experiment that has been carried out and the authors claim that the large change in the ion current when using alcohols, methanol and ethanol, may be caused by small amounts of additives in these fuels. This was seen when the alcohols were burned in an atmospheric burner, and the flame was yellow. This suggests that there were

some impurity of sodium in the alcohol fuels.

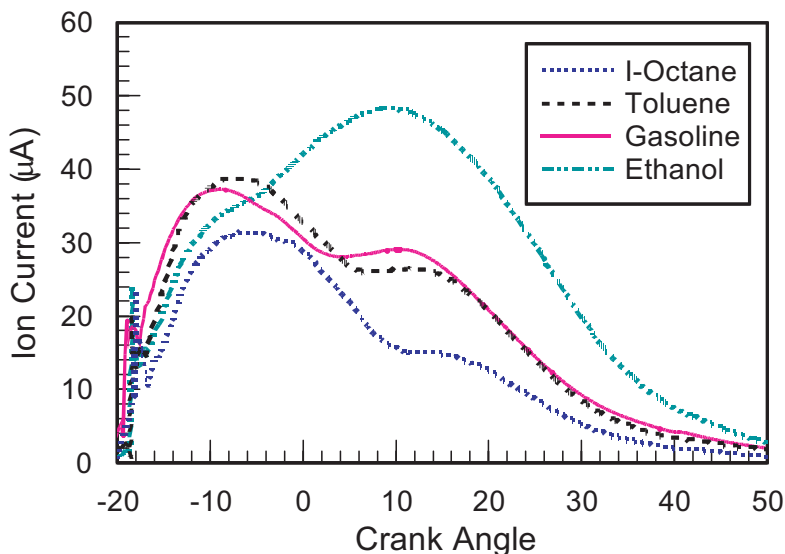


Figure 3.1: Ion currents from four different fuels, where the disturbance from the ignition has been removed, measured in the SAAB engine. The engine conditions were 2000 RPM,  $\lambda = 1.0$  and 3.5 bar BMEP. Figure 10 on page 6 in [16]. This shows a large difference in the amplitude of the signals from ethanol and gasoline, especially in the post flame phase.

If additives like potassium (K) or sodium (Na) are added to the fuel, the amplitude of the ion currents is substantially increased. These species are in the chemical group of alkali metals, and have very low ionization energy. Since much of the ions comes from the alkali metals it is hard to say anything else about the combustion. This was also experimentally tested in [16]. Additions of sodium and potassium affected both the amplitude and the shape of the ion current signal. The amplitude was about four times higher for 48 ppm Na in the fuel, than the reference. The signal also had only one peak, the first peak seemed shadowed by the very high second peak.

Another conclusion that was drawn in this paper is that the first peak is sensitive to the C/H ratio of the fuel. This is explained by different fuels form ions more or less easy in the flame due to different C/H ratios. Since the differences are in the flame, the results of this can be seen in the first peak. The C/H ratios are different for ethanol and gasoline, and the C/H ratios for some fuels can be seen in Table 1.1.

A difference in the ion current signal is also shown depending on how much aromatic hydrocarbons the fuel contained. Iso-octane which is very low aromatic has a smaller ion current and toluene which is high aromatic

has a higher current. Gasoline, that is a mixture of different hydrocarbons, both aromatic and non aromatics have an ion current signal that is between the ones for iso-octane and toluene. This can also be seen in Figure 3.1.

### 3.4 Startup Synchronization

SAAB is today using the ion currents to synchronize the engine at startup [16]. This means to determine which stroke the engine is in at the startup. This was the first application of the ion currents that was used in production cars. This information could be found in the low frequencies, below 200 Hz [4]. The startup synchronization is done by trying to ignite the gas in both the possible cylinders, and then use the ion current to see in which it has been a combustion.

### 3.5 Feedback for Ignition Timing

Since the second peak is related to the pressure, this can be used for feedback for spark advance. In [8] the ion current is used to get an estimate about the peak pressure position, and then used for determining the optimal spark advance. The benefits compared to the ordinary open loop system, are that it is possible to compensate for non-measurable disturbances such as air humidity and that the efficiency of the engine can be optimized. This can be done in real time.

### 3.6 Determining the Local Air to Fuel Ratio

Several papers that have been written on the ion currents dependence on  $\lambda$  or air to fuel ratio, see Section 2.3.3. Since the currents shows a dependence on  $\lambda$ , it would be possible to determine it from the ion currents.

In [17] the dependence of local air-fuel ratio in the vicinity of the spark plug is explained by a chemical kinetic model that uses electro-chemical reactions. First a neural network was used to see where the strongest correlation between the ion current and the oxygen sensor were. This was found in the first peak. A RON dependent chemical scheme that consists of 268 elementary reactions and 62 chemical species can describe the species concentration as a function of crank angle degrees. The conclusion in [17], is that the ion current can be used for measurements of the local  $\lambda$  in the vicinity of the spark plug with an accuracy of  $\pm 3\%$ . This can be used as a complement to the  $\lambda$  sensor. Since the ion current measures the local  $\lambda$  it can differ quite much from the  $\lambda$  sensor which is a mean value of all cylinders, it would be possible to use the ion current for feedback to the fuel injection on a cylinder basis.

In [18] an attempt to use closed loop control of  $\lambda$  using the ion current signal as feedback was made. The results were reasonable, but the estimation

were harder for rich engine operation than for lean ones. This can be used for individual  $\lambda$  control and individual diagnostics for the different cylinders in a multi cylinder engine.

### **3.7 In HCCI Engines**

In [3] the possibilities to use ion currents in homogeneous charge compression ignition, HCCI, engines, for feedback control is investigated. HCCI engines combines the best of the Diesel and the gasoline engines. The HCCI engine premixes the fuel and the oxygen and then the mix is compressed and auto ignites. This makes the engine more efficient than a gasoline engine and cleaner than a Diesel engine, but more difficult to control. This is an interesting application of ion currents for the future since this would be a cheaper way to control the HCCI engine than the pressure transducers.

# Chapter 4

## Measurements

Measurements were made in a Saab 9-3 with a 2.2l turbo engine. Indolene was used as reference fuel, and was blended with E85. E85 consists of approximate 85% ethanol and 15% 95 octane gasoline [1].

### 4.1 Ethanol Content

To get accurate results it is important to know the ethanol content in the fuel. There are two ways to determine that. One is to use (4.1). This method is sensitive to sensor errors, and since indolene has not the same stoichiometric air to fuel ratio as standard gasoline, this method is complicated. During the measurements it was concluded that this method did not give accurate results. The other method to determine the ethanol content is to use an alcohol meter. This was the method that were used because it was more reliable.

$$100\alpha \left( 1 - \frac{M_{air}}{AF_{gasoline} * M_{gasoline}} \right) \quad (4.1)$$

where

$$\alpha = \frac{AF_{gasoline}}{AF_{gasoline} - AF_{ethanol}} \quad (4.2)$$

### 4.2 Measurement Points

The measurements were done in a lab, where it was possible to control the engine speed, air mass flow, ignition timing and other parameters manually. To see the influence on speed, load and ignition timings, measurements over many operating points were done. Engine speeds from 1000 to 3000 RPM were used. Because of limited sampling rate in the measurement system, higher speeds could not be used. Air mass flows from 150 to 450 mg/c were

measured. The limitation here was the brakes. The ignition timing was varied from 8 degrees before to 8 degrees after the standard ECU ignition. In some operating points also  $\lambda$  was varied, from 0.85 to 1.0. Higher  $\lambda$  was not used since the ECU never uses lean  $\lambda$  values, due to emissions. All the operating points can be seen in Appendix B. The ion currents and cylinder pressures were sampled every CAD, for all 4 cylinders. As many operating points as possible were measured, with consideration to the limitations of the measurement system and the limited time in the lab.

### 4.3 Spark Plugs

The electrode gap size affects the ion current, see Section 2.3.4. When the spark plug gets old the gap size is changed. Older spark plugs have bigger gap because of wear. The algorithm to find the ethanol content in the fuel should work even if the spark plugs are changed, and should be robust against different spark gaps. Therefore measurements of the ion currents were done using four different spark plugs. Three were new, two of them with normal gap of 1.05mm and one with smaller gap of 0.80mm. In the last cylinder an old spark plug was used.

# Chapter 5

## Preprocessing

Some characteristics of the measurement system made it necessary to preprocess the data.

### 5.1 Normalization

Figure 5.1 shows the data before the preprocessing. The figure shows 40 cycles from the same operating point from each cylinder. What can be noted is that the amplitude of the currents differ, although they are from the same operating point. This is easiest to see in the first square of the signal, in this case from cylinder 1 and cylinder 2. This is not a result of any chemical process, instead it is a result of the equipment used for the measurements. The first square of the signal always corresponds to  $100\ \mu\text{A}$ . The measurement system changes the amplitude of the signal and therefore a normalization must be done to get back to the right values. Figure 5.2 shows the current from cylinder 1, when it has been normalized and it can be seen that all the cycles are at the same level. The normalization is done by dividing the whole cycles amplitude with the amplitude of the  $100\ \mu\text{A}$  part.

### 5.2 Synchronizing

The sampling of data started when the start button was pushed and not at any particular crank angle. To be able to put together and compare the signals they must have the same x-axis. An algorithm that found the ignition timing in every cycle was developed. The signals were synchronized so the ignition always corresponds to  $x = 0$ . Note that this implies that the signals start at ignition, and since ignitions are moving, it is not possible to directly translate this angle to crank angle. This means that TDC is not located at 0 degrees in the signals and it will be at different places when the ignitions moves.

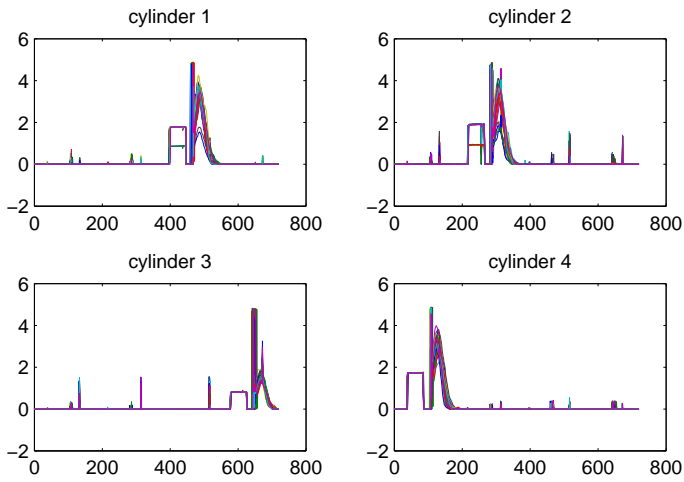


Figure 5.1: Measurements of 40 cycles. Measured with E85, 3000 RPM and 450 mg/c. There are differences in amplitude between different cylinders but also in one cylinder, although the operating point is the same. This is a result of the measurement system and the signals have to be normalized in order to be compared correctly.

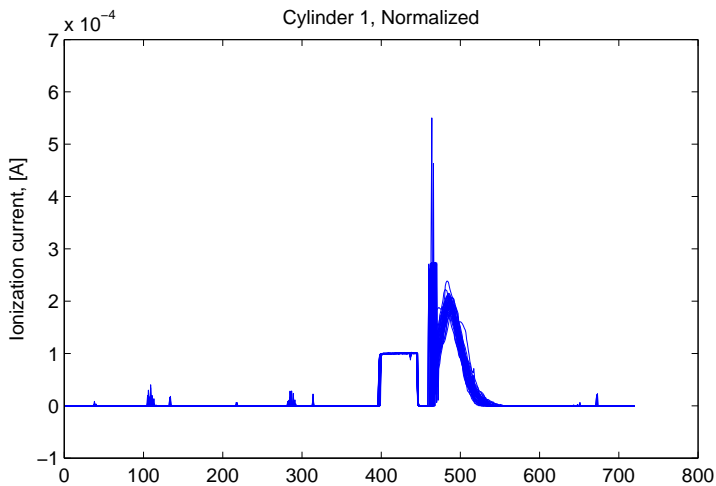


Figure 5.2: The normalized ion current of cylinder 1. All the 40 cycles now have the same amplitude, compare with Figure 5.1. Measured with E85 3000 RPM and 450 mg/c.

Because of limitations in the measurement system only 40 cycles could be measured each time. This is too little to avoid much influence of random cycle to cycle variations. Therefore several measurements were made at the same operating point. Because of the synchronizing algorithm all the sets can be put together. The algorithm cuts one cycle to make the synchronizing correct, so only 39 cycles are used from each set.

### 5.3 Filtering

The release of the spark introduces a ringing phenomena in the signal. In Figure 5.3 the ringing can be seen. The amplitude of the ringing is often larger than two times the amplitude of the rest of the signal and to avoid errors in the estimation used later this had to be filtered out. Since the ringing only was one sample in each cycle a highly non-linear filter was used. First a zero phase filter was used to flatten the signal. This was implemented using the function `filtfilt` in MATLAB. The samples in the non filtered signal that differed too much from the flattened signal were replaced by a linear interpolation between the sample before and after the removed one. A linear interpolation was used since there was only one sample at each place that should be removed. The result can be seen in Figure 5.3 and as can be seen all the ringing has been removed.

In Figure 5.1 some spikes can be seen. This is measurement noise from the ignition in the other cylinders. These spikes occurs every 180 degrees and they coincide with the ignition in the other cylinders. It can be noted that the spikes are higher in cylinder 2 and 3 than in 1 and 4. This is probably because the location of the cylinders in the engine. Cylinders 1 and 4 are on each side and cylinder 2 and 3 are in the middle. That makes cylinder 2 and 3 more sensitive to noise from the other cylinders. The same filter is used to filter out these spikes with good results.

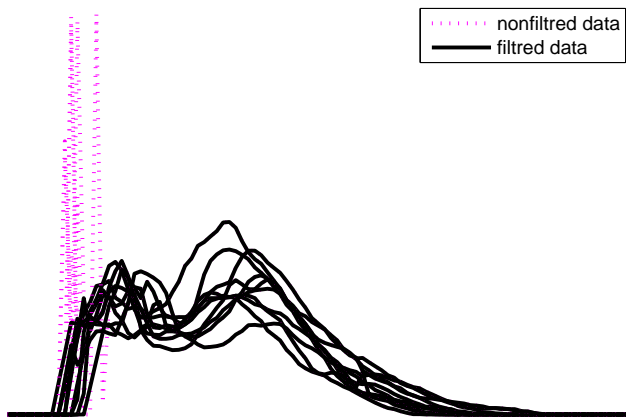


Figure 5.3: 10 cycles that shows how the ringing in the beginning of the signal is filtered out. Only the first 100 samples in each cycle are plotted.

# Chapter 6

## Qualitative Results

### 6.1 Electrode Gap Size

The spark plugs affect the ion currents and measurements were made with different spark plugs, see Section 2.3.4 and Section 4.3. Figures 6.1 - 6.3 show the ion currents from the different plugs, every curve is a mean over 40 cycles. These signals are not filtered, just moved and normalized. The three figures show different engine speeds. What can be seen in the figures is that the signals from the different spark plugs differ some in amplitude, but it does not seem like there are any clear trends. The differences between the spark plugs are in the same order of magnitude as the difference between the two identical spark plugs, cylinder 1 and 2. This implies that the differences seems to be of random cycle to cycle variations, and not a result of the spark gaps. The conclusion is that the different spark gaps do not affect the ion currents that much. The amplitude of the signals differ some from different cylinders although the spark plugs are similar. This has to be taken into account if the amplitude of the currents is used for ethanol estimation.

### 6.2 Comparison of Ignitions

Since the ignition timing affects the cylinder pressure, this is an important parameter to look at. The mistake of looking at changes from different ignitions and not to different ethanol blends should be avoided. To check if the ECU ignites the blend at different angles for different ethanol blends Figure 6.4 was made. As can be seen in the figure the ignition depends on both engine speed and torque, but not on ethanol blend, since all the markers are at the same place at each point. This assures that the ignition timing is the same for every ethanol blend, at least at the points that were measured in these data sets. The ignition can differ in high load cases, when the knock detection affects the ignition, because ethanol has a higher octane number. Since the ignition does

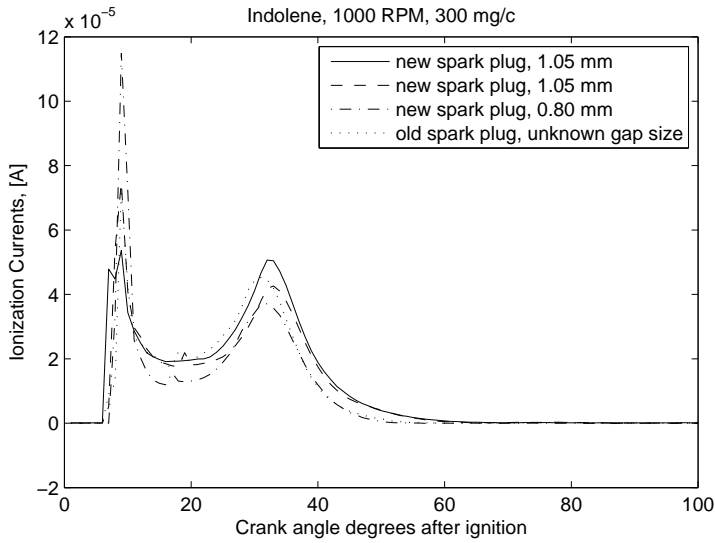


Figure 6.1: Ion current signal from different spark plugs at 1000 RPM. The signals differ some in height. Compare with Figures 6.2 and Figure 6.3. Note that the differences between all the spark plugs are in the same order as the difference between the two identical spark plugs.

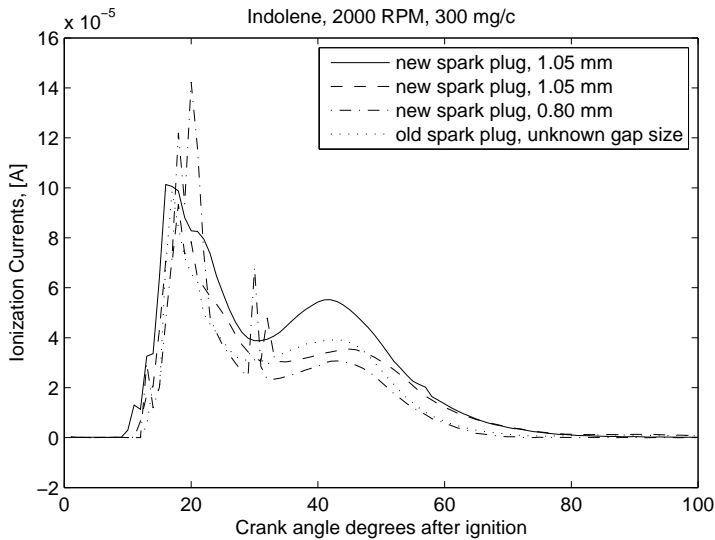


Figure 6.2: Ion current signal from different spark plugs at 2000 RPM. The signals differ some in height. Compare with Figure 6.1 and Figure 6.3. Note that the differences between all the spark plugs are in the same order as the difference between the two identical spark plugs.

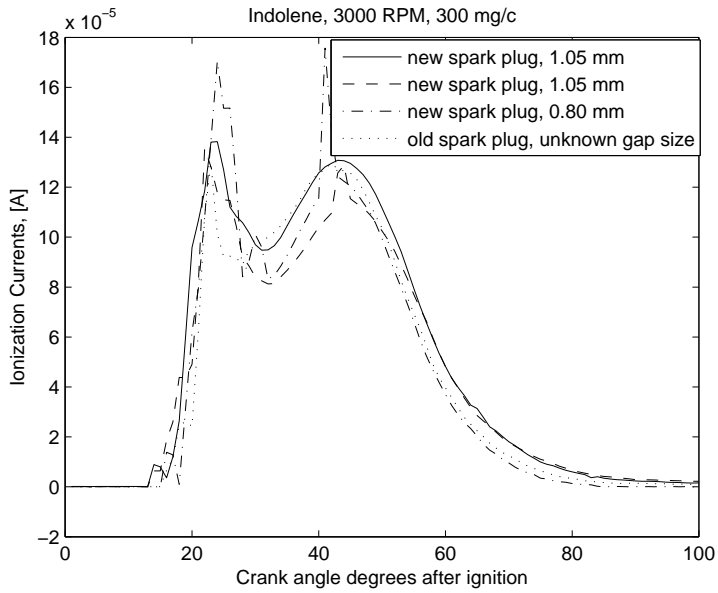


Figure 6.3: Ion current signal from different spark plugs at 3000 RPM. The signals differ some in height. Compare with Figure 6.1 and Figure 6.2. Note that the difference between all the spark plugs are in the same order as the difference between the two identical spark plugs.

not vary with ethanol content, there will be no difference to look at the ion current signals after ignition angle or after TDC. Since it will be easier to look at the signal with starting point at the ignition, this will be done in the rest of the thesis. Because the ignitions have not been checked outside these operating points, it is important to not use the ethanol estimation model outside this area. Further studies have to be made in that case.

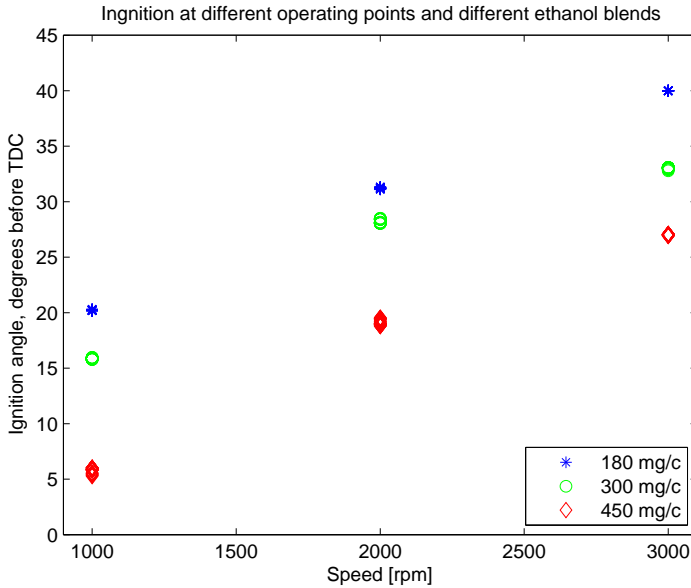


Figure 6.4: Ignition at different ethanol blends as a function of engine speed. Ignition angle as a function of speed, the different markers represent different air mass flows. The ignitions are plotted for 6 different ethanol blends, as can be seen the ignitions are the same for all the blends.

## 6.3 Air to Fuel Ratio

A comparison of the ion current for different  $\lambda$  values was done. The air to fuel ratio or  $\lambda$  affects the ion currents, see Section 2.3.3. In Figure 6.5 the ion current for different  $\lambda$  are plotted for a ethanol content of 52%.  $\lambda$  were 0.85, 0.90, 0.95 and 1.0. The ion current amplitude has a maximum for 0.85 and is the lowest for 1.0. These are the same results as in [16] for gasoline, cf. Figure 2.2. Since the order of the ion currents are the same in both operating points and these results have been found in [16] for gasoline, the conclusion is that the  $\lambda$  dependence is the same for ethanol-gasoline blends as for gasoline.

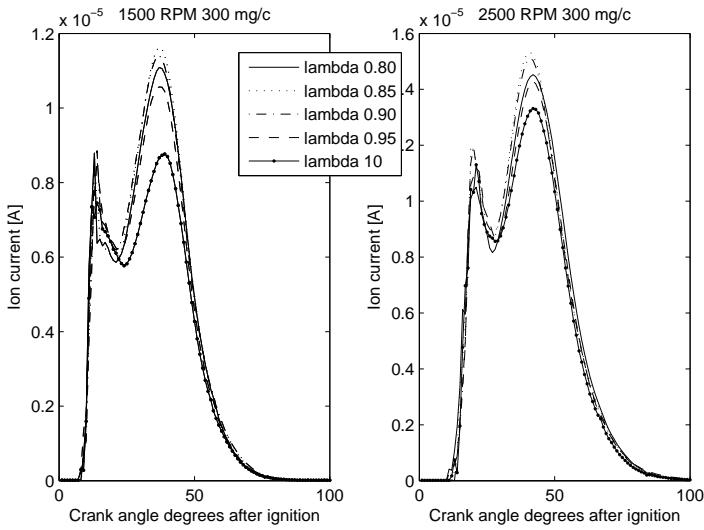


Figure 6.5: Ion current plotted for different  $\lambda$  from 0.85 to 1.0, means over 117 cycles, all from the same cylinder.  $\lambda = 0.85$  has the highest amplitude. The differences are not that big, but this is the same result as in [16]. Since the order is the same in both operating points and literature explains these  $\lambda$  dependences, it is concluded that the  $\lambda$  dependence is the same for ethanol-gasoline blends as for gasoline. Compare with Figure 2.2.

## 6.4 Ethanol Content

To see if there are any differences in the ion currents from different ethanol ratios, the signals from four different ethanol blends were plotted. The result can be seen in Figure 6.6. The ethanol contents are 0%, 9.0%, 24.5% and 84.5%. It is hard to see any trend about the ethanol content but the load and speed affect the currents. The differences between the ethanol contents are not that big as the differences between the operating points. The differences could be due to random cycle to cycle variations and not at all a result of the fuel blending. It was hard to see anything at all, when just plotting the signals and therefore some quantitative investigations was motivated.

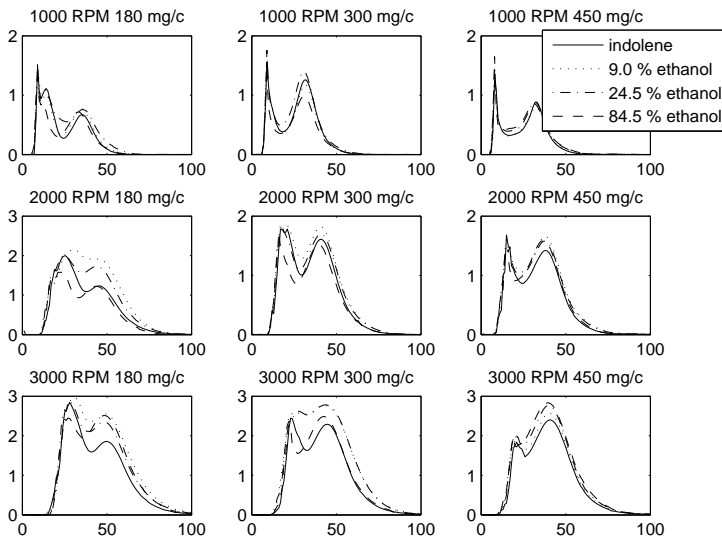


Figure 6.6: Comparison of ion currents for different ethanol blends. The figure shows means over 195 cycles, and are all from the same cylinder. The ion currents depend mostly on load and speed, and some on ethanol content. There are not any clear trends about the ethanol content.

# Chapter 7

## Quantitative Results

The search for trends depending on ethanol content was hard, as shown in Chapter 6. Since it is not possible to see any direct apparent connection, a model for the ion current signal is needed. In this chapter a Gaussian model that estimates parameters from the ion currents is described. A black box model for these parameters dependence on speed, load and ignition timing is presented and evaluated.

### 7.1 Modeling

#### 7.1.1 The Gaussian Model

There are several available models describing the ion current. In [8] a model is used that approximates the signal with two Gaussian functions, one for each peak. The model for the ion current becomes

$$I(\theta, \bar{\alpha}) = \alpha_1 e^{-\frac{1}{\alpha_2}(\theta - \alpha_3)^2} + \beta_1 e^{-\frac{1}{\beta_2}(\theta - \beta_3)^2} \quad (7.1)$$

where  $\theta$  is the crank angle and  $\bar{\alpha}$  is the parameter vector

$$\bar{\alpha} = (\alpha_1, \alpha_2, \alpha_3, \beta_1, \beta_2, \beta_3)$$

The parameters can be interpreted as

- $\alpha_1$  height of the first peak
- $\alpha_2$  width of the first peak
- $\alpha_3$  position of the first peak
- $\beta_1$  height of the second peak
- $\beta_2$  width of the second peak
- $\beta_3$  position of the second peak

With this model trends can be seen in the parameters that are hard to see when just looking at the plots of the signals. After the preprocessing of the data, see Chapter 5, the signal can be estimated, with (7.1). For this the command `lsqnonlin` in MATLAB was used and an example of the results can be seen in Figure 7.1. When the signals are filtered the algorithm for finding

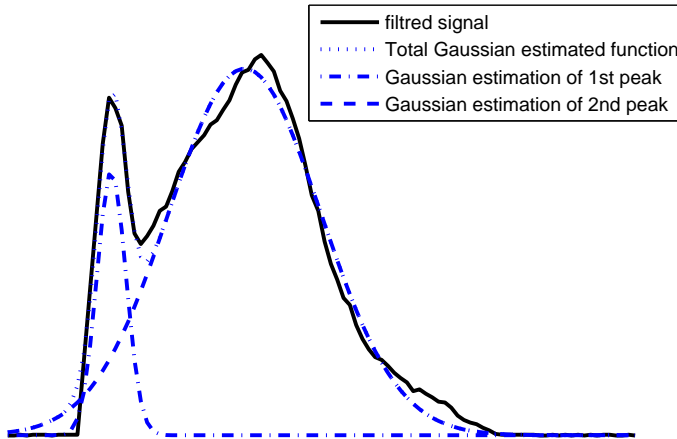


Figure 7.1: The signal and the two estimated Gaussian functions. The estimation agrees very well with the signal.

the Gaussian functions finds the two peaks if the start values are quite close to the right ones. To get an initial guess of what the parameters should be some testing was made, and the fact that all the signals have a similar shape, although quite large cycle to cycle variations exist was used. The parameters  $\alpha_1$  and  $\beta_1$ , the height of the peaks, are set to the maximum value of the signal, and all the other start values were found by testing. This start guess gave good results on almost all of the signals. After the parameters have been estimated, a manual check of many of the signals were made, to ensure that the estimation found reasonable values. The result of this check was that a few estimates found wrong values, but most of the cycles had converged to reasonable values. The few that did not converge to reasonable values were often the signals that did not have a clear first peak. In Figure 7.2 an estimation that found unreasonable values can be seen. Since the unreasonable ones were that few, and almost all were right, the decision was taken that this would not affect the mean value of the 117 cycles that would be used in the model. In Figure 7.3 all the estimated values for engine speed 2000 RPM and

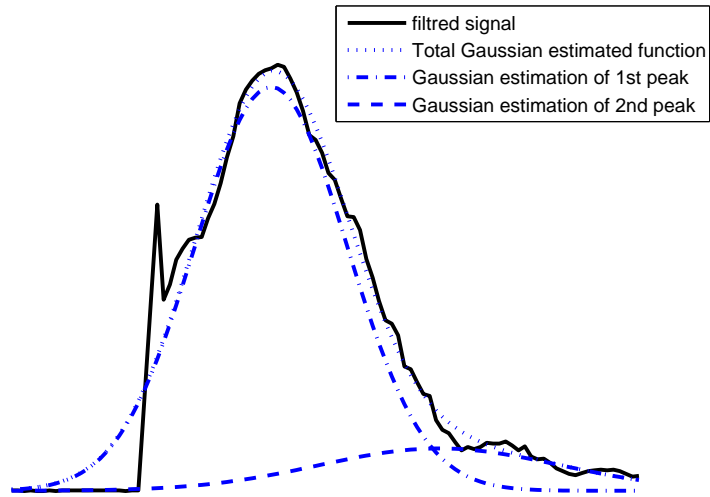


Figure 7.2: An example of a Gaussian estimation that did not find reasonable values

air mass flow 300 mg/c can be seen. There are a few outliers, but using the mean value is motivated by that the most of the estimations are right. A filter that removes the outliers would be a way to get rid of the wrong ones. This has not been done but would be a possible improvement for future use.

Since the ethanol content in the fuel is not changed often, at the most every time the car is fueled, the choice of using the mean value is motivated. The algorithm that would find the ethanol content would not run all the time, just when the engine is running in steady state, as soon as possible after fueling. To compensate the model for dynamics in the engine seemed complicated and unnecessary. This is because every driver runs the engine in steady state at some instances between every fueling, and 117 cycles are not that many seconds. For instance, at idle speed this would correspond to less than 9 s.

The parameters that were estimated were used to see if there were any dependencies on ethanol content. It was hard to see any trends in these parameters that were valid for all speed and load cases. The variations between operating conditions were large, and to decouple these effects a model had to be made for how the six model parameters depended on the operating point of the engine. The idea was to make a black box model of the known quantities speed, load and ignition timing to be able to decouple the variations that just depended on those.

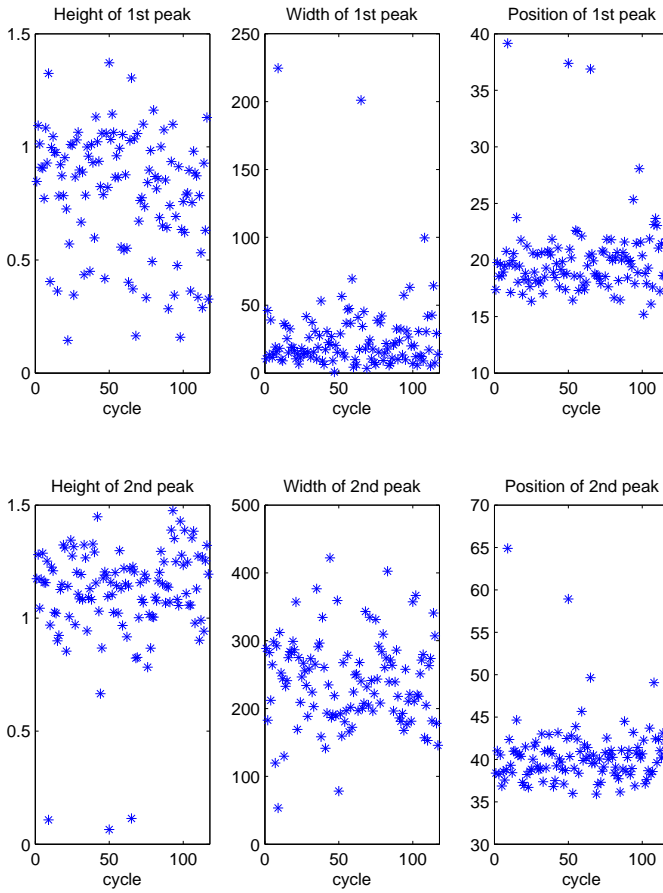


Figure 7.3: The Gaussian estimations of all the cycles at 2000 RPM and air mass flow 300 mg/c. A few outliers can be seen.

### 7.1.2 Black Box Model

A black box model for the ion currents dependence on speed, load and ignition timing was developed. The six parameters from the Gaussian model was assumed to be a quadratic function of the known parameters, see (7.2).

$$\bar{\alpha}_i = x_{i1} + x_{i2}S + x_{i3}S^2 + x_{i4}L + x_{i5}L^2 + x_{i6}I + x_{i7}I^2 + x_{i8}SL + x_{i9}SI + x_{i10}IL \quad (7.2)$$

$$\bar{x}_i = \begin{pmatrix} x_{i1} \\ x_{i2} \\ x_{i3} \\ x_{i4} \\ x_{i5} \\ x_{i6} \\ x_{i7} \\ x_{i8} \\ x_{i9} \\ x_{i10} \end{pmatrix}$$

where

- $\bar{\alpha}$  : The vector with the six parameters from the Gaussian estimation, see (7.1)
- $S$  : The speed
- $L$  : The load
- $I$  : The ignition timing
- $\bar{x}_i$  : The model parameters

The model parameters  $\bar{x}$  were estimated with the least square method in MATLAB for 52% ethanol. 52% ethanol was chosen since it is in the middle of the ethanol ratios. The mean value of the 117 cycles was used, to avoid the cycle to cycle variations. 61 operating points were used do the estimation, of the ten model parameters for each  $\alpha_i$ . Total 60 model parameters were estimated, for  $\bar{\alpha}$ . Because 6 values from every operating point could be used, total of 366 values, this was enough for estimate the 60 parameters.

Since all the data are crank angle based, and not time based, this model will be crank angle based. The linear term of the engine speed will describe the dependencies that are time based. The ion current position speed dependence are almost constant in time, but it will be linear in this crank angle based model.

## 7.2 Evaluation

In this section the model and the dependences on and speed, load, ignition timing and ethanol content are evaluated. The model is compared to the measured values. Measured values are the estimations from the Gaussian model

in Section 7.1.1, and modeled values are the estimations from the black box model in Section 7.1.2. As can be seen in this section the model approximates the measured values quite well.

### 7.2.1 Speed Dependencies

The results of the model estimation of this can be seen in Figure 7.4 where the model and the measured data are plotted as a function of engine speed. For clarity, only the ECU standard ignition timing is plotted instead of all five that are used in the parameter estimation. Since Figure 7.4 is a little bit messy, Figure 7.5 shows the same thing for just air mass flow of 300 mg/c. As can be seen in the figures the model approximates the measured values quite well. Another thing that can be noted in the figures is that the position of the peaks are increased almost linear with the speed. Every CAD corresponds to shorter time when the engine runs faster. Note that this is the position of the peaks relative to the ignition timing. The difference due to the engine speed is about 15 degrees, between 1000 and 3000 RPM. Compare this figure with Figure 6.4, where it can be seen that the ignition timing differs approximately 15-20 CAD. The 3000 RPM speed sets are ignited earlier than the 1000 RPM, and the ion current position are later. The conclusion is that the peaks probably are in the same position relative to TDC, but the position increases with speed relative to ignition timing.

Figure 7.4 also shows that the width of the peaks increases with speed. The same explanation as for the positions is valid here too. Also the height of the peaks increases with increased speed.

### 7.2.2 Load Dependence

The same thing as in Figure 7.4 are shown in Figure 7.6 and Figure 7.7, but instead of speed the data are now plotted as a function of air mass flow. These figures also show that the model agrees well with the data. The dependence on load is not that clear as in the speed case, but it can be seen that the height of the second peak increases with load. This is in agreement with Section 2.3.1. When the load is increased, more air-fuel mixture is burned, and therefore the cylinder pressure and temperature rise, and so also the amplitude of the second ion current peak.

The positions of the peaks,  $\alpha_3$  and  $\beta_3$ , decrease with the load. The ignition timing is later for higher loads, and the ion current peak is earlier relative to the ignition timing. Compare with Figure 6.4. This means that the positions here also are at the same place relative to TDC, but decrease relative to the ignition timing.

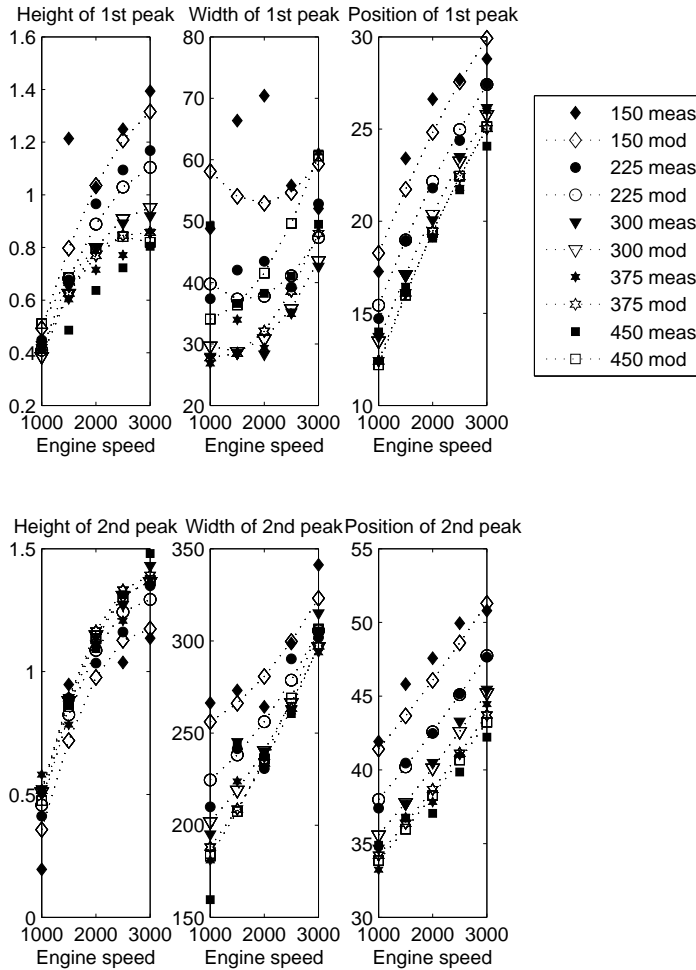


Figure 7.4: The model and the mean values of the measurements for 52% ethanol as a function of engine speed, for five different air mass flows. Meas is measured mean value of 117 cycles and mod is model. The numbers in the legend are the air mass flows in mg/c. The model and the measurements agree well. Note the dependence on speed.

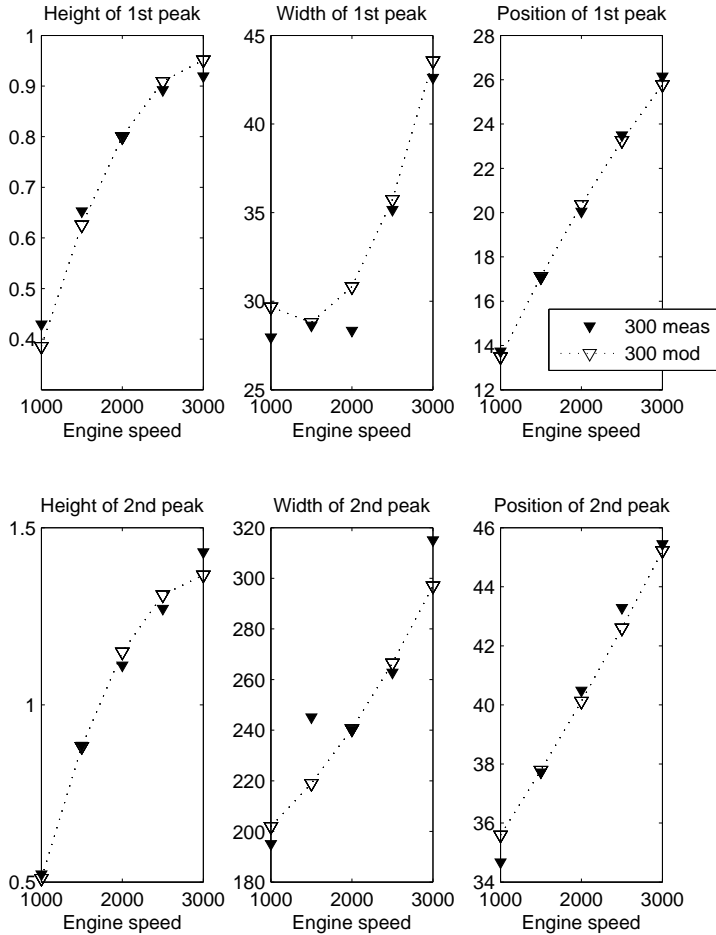


Figure 7.5: The model and the mean values of the measurements for 52% ethanol as a function of engine speed for the air mass flow of 300 mg/c. Meas is measured mean value of 117 cycles and mod is model. Compare with Figure 7.4. This figure shows more clearly how the model and the measurements agree.

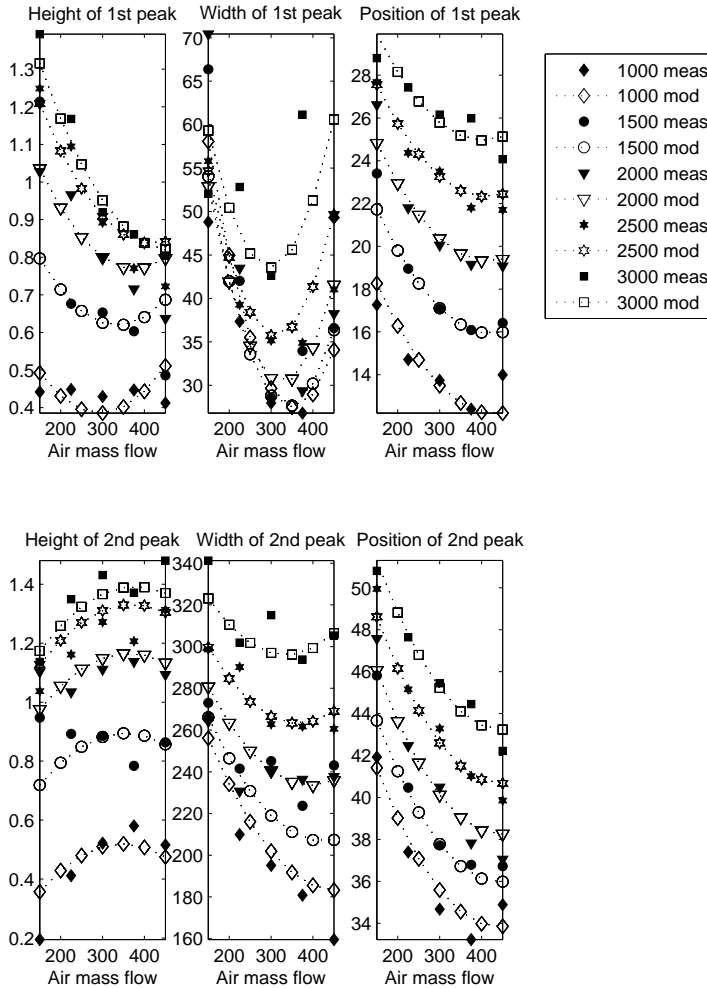


Figure 7.6: The model and the mean values of the measurements for 52% ethanol as a function of air mass flow, for five different engine speeds. Meas is measured mean value of 117 cycles and mod is model. The numbers in the legend are the speeds in RPM. The height of the second peak increases with load.

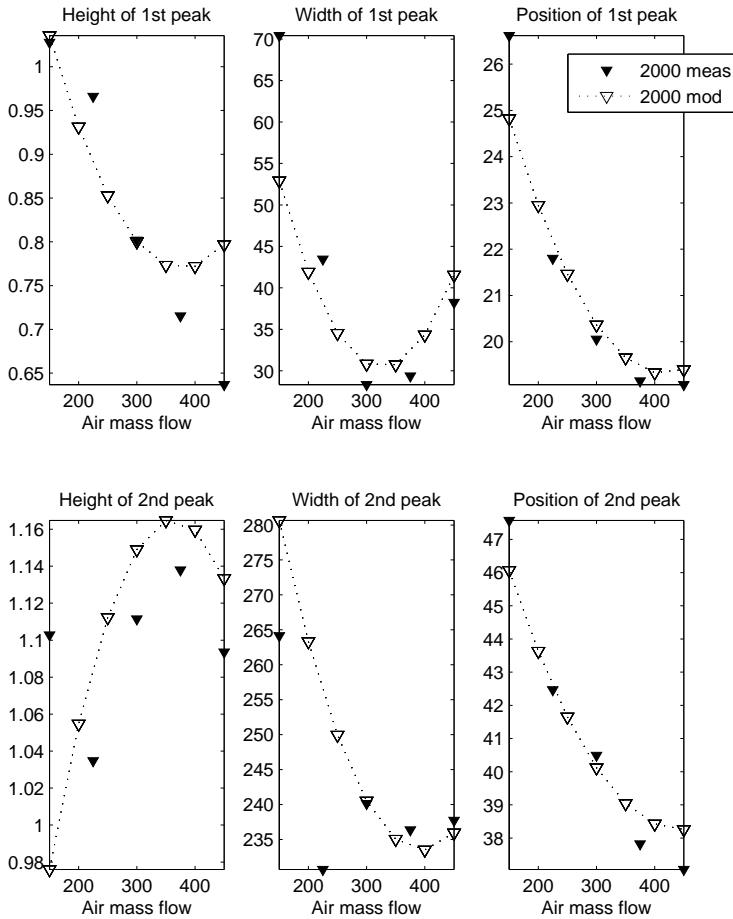


Figure 7.7: The model and the mean values of the measurements for 52% ethanol as a function of air mass flow, at a speed of 2000 RPM. Compare with Figure 7.6. The model estimates the data well.

### 7.2.3 Ignition Dependencies

Figure 7.8 and Figure 7.9 show how the model parameters depend on the ignition timing. The position and width are almost constant when the ignition timing is changed. The position is relative to the ignition timing and not to TDC, see Section ???. The combustion takes approximately the same time from ignition to end, regardless of the ignition timing, if the load and engine speed are the same. The only parameters that seem to be affected by the ignition timing are the height of the peaks, they increase some with earlier ignitions. This is a result of that the ignition timing affects the cylinder pressure.

### 7.2.4 Ethanol Dependencies

Since the main objective in this thesis is to estimate the ethanol ratio, the dependence on ethanol is interesting. If there are any significant differences between the datasets with the two ethanol blends 52% and 85%, such a dependence can be used to detect different ethanol blends. Figure 7.10 shows the difference between the model and the measured values for both 52% and 85% ethanol. If the dots would divide into two different groups, depending on the ethanol content there would be a significant difference between them. Then it would be a difference between the ethanol blends that would show when the known quantities, speed, load and ignition timing are decoupled. The figure is a bit messy, but sometimes the 52% has higher values and sometimes 85% has the higher values. Since the result varies with operating point, the model describes both datasets equally. Since the variations from operating point are modeled away a dependence of ethanol content will show in the same way in all operating points.

Even since the ignition timing is just the normal the two sets can not be separated. Note that in the figure the mean values of 117 cycles are plotted, and there is still overlap between the two blends. If all the values are plotted the overlap is of course bigger. The two blends of ethanol can not be separated and therefore the conclusion is that the black box model can not be used for ethanol estimation. Since the difference in ethanol content is quite large, finding an algorithm that can separate blends this way seems very hard.

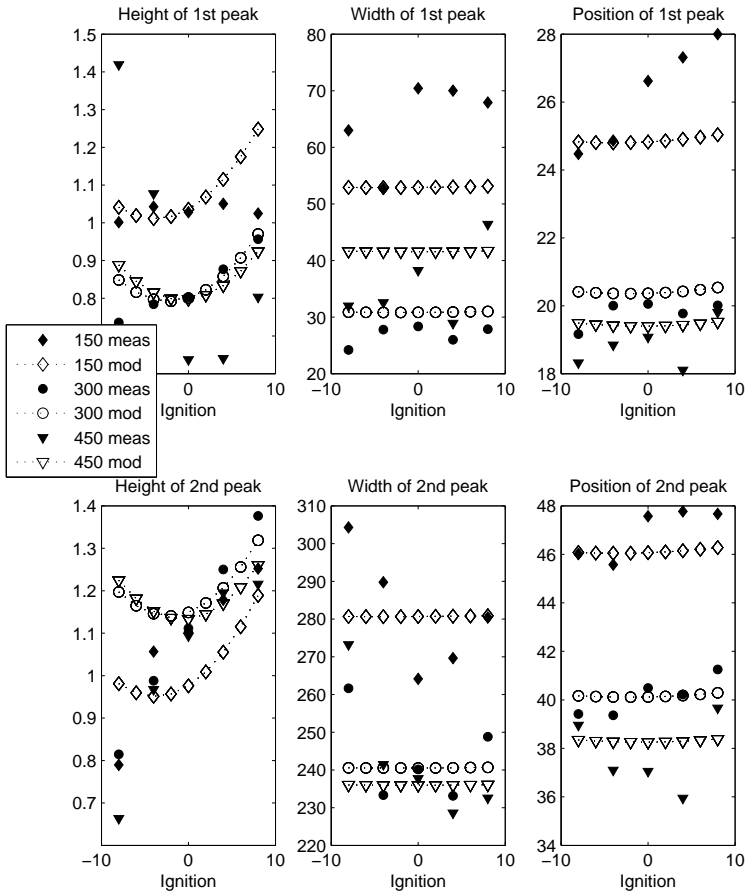


Figure 7.8: The model and the mean values of the measurements for 52% ethanol as a function of ignition timing, speed 2000 RPM. The different markers are different air mass flows in mg/c. Meas is measured mean value of 117 cycles and mod is the model. Ignition is degrees relative to the ECU ignition in CADs before TDC. -8 means an ignition timing 16 degrees closer to TDC than +8. Only the heights of the peaks vary with the ignition timing, since cylinder pressure is affected by the ignition angle.

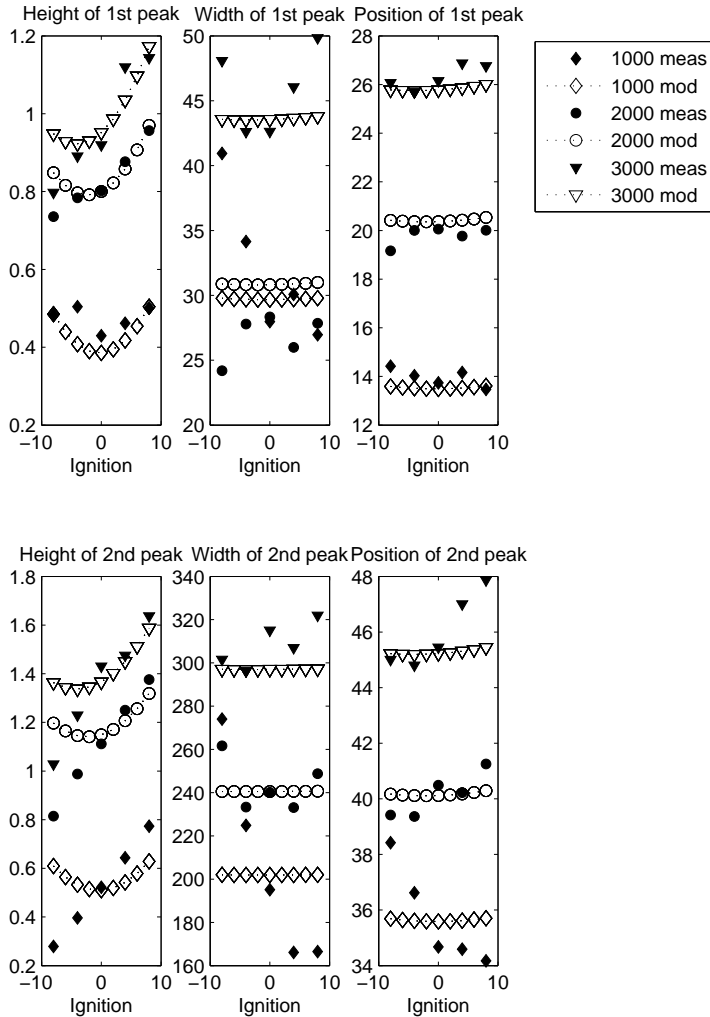


Figure 7.9: The model and the mean values of the measurements for 52% ethanol as a function of ignition timing, air mass flow of 300 mg/c. The different markers are different engine speeds, in RPM. Meas is measured mean value of 117 cycles and mod is the model. Ignition is degrees relative to the ECU ignition in CADs before TDC. -8 means ignition timing 16 degrees closer to TDC than +8.

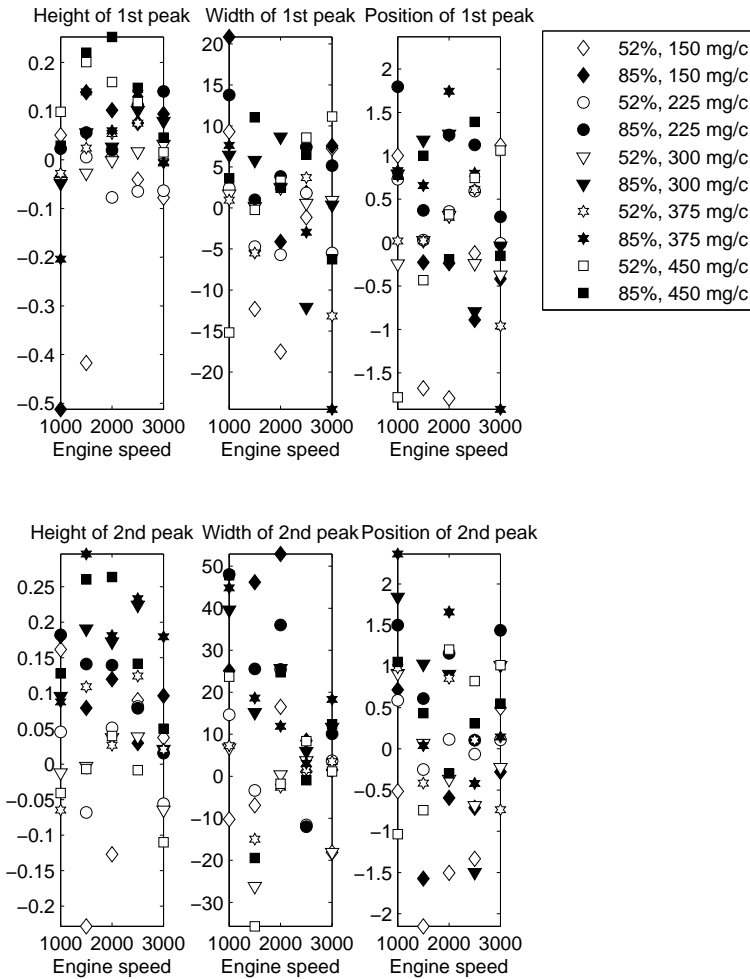


Figure 7.10: The modeled value minus the measured mean values as a function of speed for five different loads, both 52% and 85% ethanol. The figure shows five loads at each speed. Since the two ethanol blends can not be separated, the model corresponds as well for 85% for 52% ethanol. Since the model was made for 52%, it can not be used to estimate the ethanol ratio.

### Relative Errors and Mean Square Errors

To further investigate if there is some difference between two ethanol blends the relative error and the mean square error were calculated. The relative error, between modeled and measured values, can be seen in Figure 7.11. The relative error is calculated as:

$$e(k) = \frac{meas - mod}{meas} \quad (7.3)$$

The two data sets, 52% and 85%, seem to have similar relative errors. Compare the heights of the peaks with Figure 7.12, where the absolute errors can be seen. Since the absolute error are approximately of the same size in all operating points, the relative error becomes large when the value is low.

The mean square error is a measure of how well the model describes the data, and is defined as (7.4).

$$mse = \frac{1}{Q} \sum_{k=1}^Q e(k)^2 \quad (7.4)$$

where In Figure 7.13 the mean square errors, between the measured and mod-

- $mse$  : Mean square error.
- $Q$  : The number of operating points.
- $e(k)$  : The relative error at operating point  $k$ .

eled values, are plotted as a function of ethanol blend and cylinder number. In these two cylinders both the spark plugs are new, and have the same spark gap. Despite this, the relative mean square errors differs from the different cylinders. What can be noted in Figure 7.13 is that the difference between the two blends, is in the same magnitude as the difference between the two cylinders with the same ethanol blend. The high relative error of  $\beta_1$  is caused by the low values that  $\beta_1$  has for low speeds and loads. This figure is included to illustrate the differences between the different cylinders and different ethanol blends. At first, it might seem like the height of the second peak differs more depending on ethanol content than on cylinder number. However, a comparison with cylinder 4, shown in Figure 7.14, shows that this is not true because this parameter also varies between different cylinders.

The conclusion is that this model can not be used to detect differences in the ethanol content since the differences between ethanol content have approximately the same size as the differences between the cylinders.

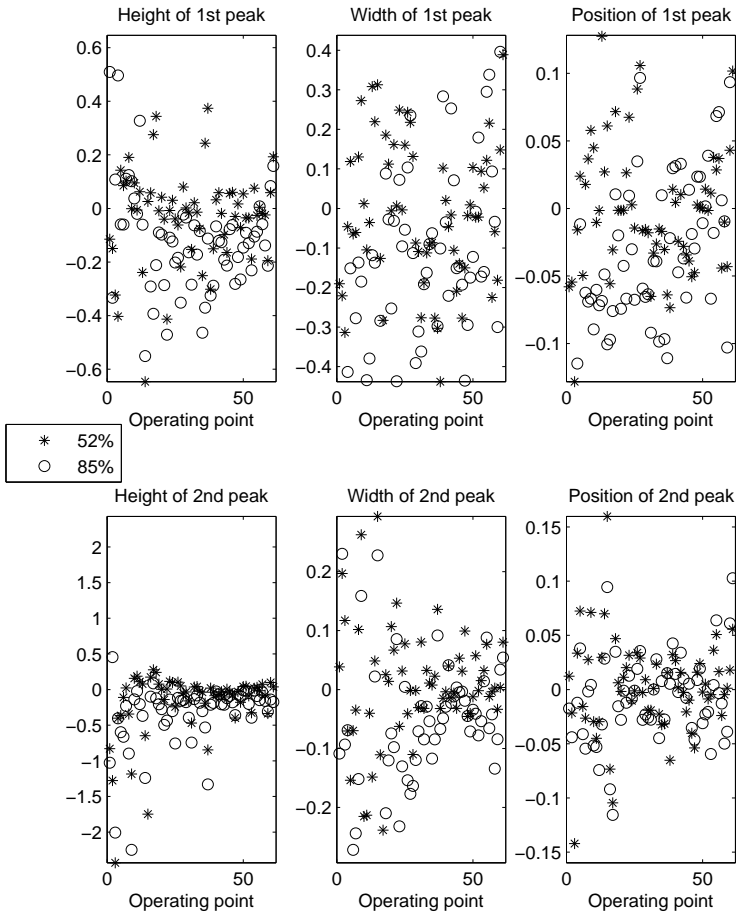


Figure 7.11: The relative error for all the parameters. For small values of the height of the second peak the relative error is large, but the others have low relative errors. All the data is from cylinder 1.

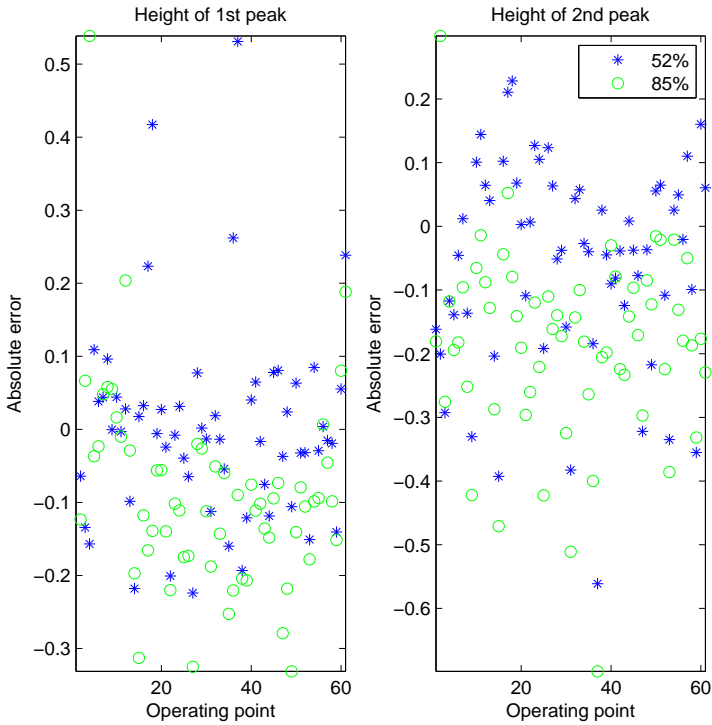


Figure 7.12: The absolute error between measured and modeled values for the two ethanol blends. All the data are from cylinder 1.

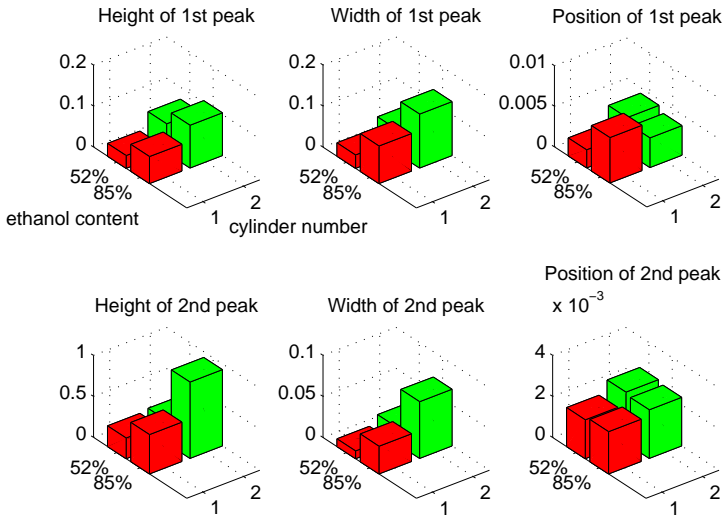


Figure 7.13: The mean square error as a function of ethanol content and cylinder number. In cylinder 1 and 2 the spark gaps are the same, but the result differs in the same order of magnitude as for the two ethanol blends.

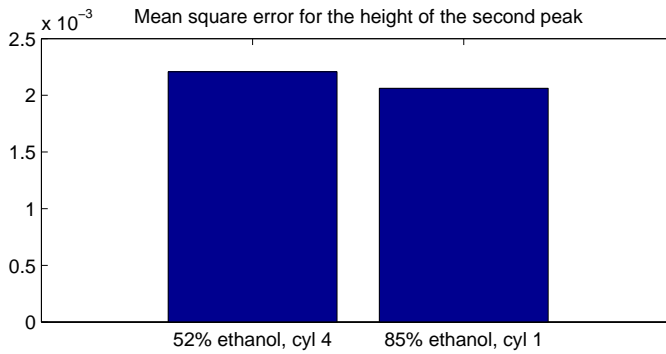


Figure 7.14: Compare with Figure 7.13. This figure shows that the mean square error of the second peak are higher for 52% in cylinder 4, than for 85% for cylinder 1. In Figure 7.13, it might seem like the differences in the height of the second peak are very large due to ethanol content and that it increases with ethanol content. This figure shows that this is not the case.

## Chapter 8

# Conclusions and Future Work

The main conclusion is that it is not possible to estimate the ethanol content in the fuel from ion currents using the suggested black box model. This has been investigated both qualitatively and quantitatively. A Gaussian function estimation of the ion current with six parameters was used. A black box model for how these parameters depend on speed, load and ignition timing was made. Even if it was quite a simple model it describes the Gaussian model parameters very well. The results indicates that the ion currents are much more affected by the operating point than the ethanol content. The difference from the ethanol content is in the same order as the differences between the cylinders in the same engine. It is also concluded that the effect of different spark plugs is not important. The two cylinders that had identical spark plugs differ in the same order of magnitude as the ones with different spark plugs.  $\lambda$ , ignition timing, load and speed dependences were concluded to be the same for ethanol-gasoline blends, as the ones found in literature for gasoline.

### 8.1 Fulfilled Objectives

The objectives of this thesis have been partially fulfilled. It has been investigated if the ethanol content in the fuel could be estimated from ion currents. The conclusion is drawn that it can not be done in any of the ways that are suggested in this thesis. This was the main objective and it has been fulfilled. Also a literature review has been done. Since it was not possible to estimate the ethanol content, no algorithm has been developed, and the other objectives about a real time implementation have not been fulfilled.

## **8.2 Future Work**

Since the conclusion is that a black box model could not capture any difference of different ethanol blends, a possibility for the future would be to use an analytical model instead.

### **8.2.1 The Analytical Model**

In [9] an analytical model for the ion current based on the cylinder pressure is presented. A future study could be to see if the analytical model predicts any differences in the ion currents from ethanol and gasoline. Since the cylinder pressure is not available in production cars today, this approach might not lead to an algorithm that is possible to implement, but it would still be interesting to evaluate.

# References

- [1] Statoil Etanol E85. internet. [http://www.statoildetaljhandel.se/file\\_archive/produktinformation/Etanol\\_E85.pdf](http://www.statoildetaljhandel.se/file_archive/produktinformation/Etanol_E85.pdf).
- [2] A. Ahmed, F. Mauss, and B. Sundén. Analysis of extended ionization equilibrium in the post-flame gases for spark ignited combustion. Technical report, Department of heat and power engineering, Lunds University, Lund, Sweden.
- [3] Hans Aulin and Pascal Bentioulis. Improving ion current feedback for HCCI engine control. Master's thesis, Division of Combustion Engines, Department of Energy Science, Lund University, Lund, Sweden, 2006.
- [4] John Auzins, Hasse Johansson, and Jan Nytomt. Ion-gap sense in misfire detection, knock and engine control. In *Society of Automotive Engineers*, number 95004, Detroit, Michigan, February-March 1995.
- [5] K. N. C. Bray and N. Collings. Ionization sensors for internal combustion engine diagnostics. *Endeavour, New Series*, 15(1):10–12, 1991.
- [6] Wen Dai, Sreeni Cheemalamarri, Eric W. Curtis, Rihadh Boussarsar, and Richard K. Morton. Engine cycle simulation of ethanol and gasoline blends. In *Society of Automotive Engineers*, number 2003-01-3093, 2003.
- [7] Gregory W. Davis and Edward T. Heil. The development and performance of a high blend ethanol fueled vehicle. In *Society of Automotive Engineers*, number 2000-01-1602, 2000.
- [8] Lars Eriksson. *Spark Advance Modeling and Control*. Phd thesis 580, Department of Electrical Engineering, Linköpings Universitet, Linköping, Sweden, April 1999.
- [9] Lars Eriksson and Lars Nielsen. Towards on-board engine calibration with feedback control incorporating combustion models and ion-sense. *Automatisierungstechnik*, (5):204–212, 2003.
- [10] Lars Eriksson and Lars Nielsen. *Vehicular Systems*. 2006.

- [11] A. Franke, W. Koban, J. Olofsson, C. Schulz, W. Bessler, R. Reinmann, A. Larsson, and M. Aldén. Application of advanced laser diagnostics for the investigation of ionization sensor signal in a combustion bomb. July 2005.
- [12] Thommy Jakobsson. Modeling of an UEGO. Master's thesis, Department of Electrical Engineering, Linköpings Universitet, Linköping, Sweden, 2006.
- [13] M. Krämer and K. Wolf. Approaches to gasoline engine control involving the use of ion current sensory analysis. In *Society of Automotive Engineers*, number 905007, 1990.
- [14] Yutaka Ohashi, Wataru Fukui, and Atsushi Ueda. Application of vehicle equipped with ionic current detection system for the engine management system. In *Society of Automotive Engineers*, number 970032, 1997.
- [15] Raymond Reinmann. *Theoretical and Experimental Studies of the formation of Ionized Gases in Spark Ignition Engines*. PhD thesis, Department of Combustion Physics, Lund University, Lund, Sweden, 1998.
- [16] Raymond Reinmann, André Saitzkoff, Bengt Lassesson, and Petter Strandh. Fuel and additive influence on the ion current. In *Society of Automotive Engineers*, number 980161, 1998.
- [17] Raymond Reinmann, André Saitzkoff, and Fabian Mauss. Local air-fuel ratio measurements using the spark plug as an ionization sensor. In *Society of Automotive Engineers*, number 970856, 1999.
- [18] Devesh Upadhyay and Giorgio Rizzoni. AFR control on a single cylinder engine using the ionization current. In *Society of Automotive Engineers*, number 980203, 1998.
- [19] Edward A. VanDyne, Charles L. Burkmyer, Alexandre M. Wahl, and Alberto E. Funaioli. Misfire detection from ionization feedback utilizing the smartfire plasma ignition technology. 2000.
- [20] Y Yacoub, R Bata, and M Gautam. The performance and emission characteristics of  $C_1 - C_5$  alcohol-gasoline blends with matched oxygen content in a single-cylinder spark ignition engine. *IMEchE*, 1998.

# Appendix A

## Abbreviations

BDC	Bottom dead center
CAD	Crank angle degrees
C/H	Carbon hydrogen ratio
ECU	Engine control unit
HCCI	Homogeneous charge compression ignition
OBD	On board diagnostics
RON	Research octane number
RPM	Revolutions per minute
RVP	Reid vapor pressure
SI	Spark ignited
TDC	Top dead center

# Appendix B

## Measurements

Many different speeds, loads, ignition timings and  $\lambda$ -values were measured. The operating points that were used are shown in Table B.1. In both the  $\lambda$  and the ignition column - means that the ECU decides the values.

<b>speed</b> RPM	<b>air mass flow</b> mg/c	<b>ignition</b> deg relative to the ECU	$\lambda$
1000	150	-8	-
1000	150	-4	-
1000	150	-	-
1000	150	+4	-
1000	150	+8	-
1000	225	-	-
1000	300	-8	-
1000	300	-4	-
1000	300	-	-
1000	300	+4	-
1000	300	+8	-
1000	375	-	-
1000	450	-8	-
1000	450	-4	-
1000	450	-	-
1000	450	+4	-
1000	450	+8	-
1500	150	-	-
1500	225	-	-
1500	300	-	1.00
1500	300	-	0.80
1500	300	-	0.85
1500	300	-	0.90

Continued on next page

**Table B.1 – continued from previous page**

<b>speed</b>	<b>air mass flow</b>	<b>ignition</b>	$\lambda$
1500	300	-	0.95
1500	375	-	-
1500	450	-	-
1750	150	-	-
1750	225	-8	-
1750	225	-4	-
1750	225	-	-
1750	225	+4	-
1750	225	+8	-
1750	300	-	-
1750	375	-	-
1750	450	-	-
2000	150	-8	-
2000	150	-4	-
2000	150	-	-
2000	150	+4	-
2000	150	+8	-
2000	225	-	-
2000	300	-8	-
2000	300	-4	-
2000	300	-	-
2000	300	+4	-
2000	300	+8	-
2000	375	-	-
2000	450	-8	-
2000	450	-4	-
2000	450	-	-
2000	450	+4	-
2000	450	+8	-
2250	150	-	-
2250	225	-	-
2250	300	-	-
2250	375	-8	-
2250	375	-4	-
2250	375	-	-
2250	375	+4	-
2250	375	+8	-
2250	450	-	-
2500	150	-	-
2500	225	-	-
2500	300	-	1.00

Continued on next page

**Table B.1 – continued from previous page**

<b>speed</b>	<b>air mass flow</b>	<b>ignition</b>	<b><math>\lambda</math></b>
2500	300	-	0.80
2500	300	-	0.85
2500	300	-	0.90
2500	300	-	0.95
2500	375	-	-
2500	450	-	-
3000	150	-8	-
3000	150	-4	-
3000	150	-	-
3000	150	+4	-
3000	150	+8	-
3000	225	-	-
3000	300	-8	-
3000	300	-4	-
3000	300	-	-
3000	300	+4	-
3000	300	+8	-
3000	375	-	-
3000	450	-8	-
3000	450	-4	-
3000	450	-	-
3000	450	+4	-
3000	450	+8	-

Table B.1: Measurement points



## Copyright

### Svenska

Detta dokument hålls tillgängligt på Internet - eller dess framtida ersättare - under en längre tid från publiceringsdatum under förutsättning att inga extraordinära omständigheter uppstår.

Tillgång till dokumentet innebär tillstånd för var och en att läsa, ladda ner, skriva ut enstaka kopior för enskilt bruk och att använda det oförändrat för ickekommersiell forskning och för undervisning. Överföring av upphovsrätten vid en senare tidpunkt kan inte upphäva detta tillstånd. All annan användning av dokumentet kräver upphovsmannens medgivande. För att garantera äktheten, säkerheten och tillgängligheten finns det lösningar av teknisk och administrativ art.

Upphovsmannens ideella rätt innefattar rätt att bli nämnd som upphovsman i den omfattning som god sed kräver vid användning av dokumentet på ovan beskrivna sätt samt skydd mot att dokumentet ändras eller presenteras i sådan form eller i sådant sammanhang som är kränkande för upphovsmannens litterära eller konstnärliga anseende eller egenart.

För ytterligare information om Linköping University Electronic Press se förlagets hemsida: <http://www.ep.liu.se/>

### English

The publishers will keep this document online on the Internet - or its possible replacement - for a considerable time from the date of publication barring exceptional circumstances.

The online availability of the document implies a permanent permission for anyone to read, to download, to print out single copies for your own use and to use it unchanged for any non-commercial research and educational purpose. Subsequent transfers of copyright cannot revoke this permission. All other uses of the document are conditional on the consent of the copyright owner. The publisher has taken technical and administrative measures to assure authenticity, security and accessibility.

According to intellectual property law the author has the right to be mentioned when his/her work is accessed as described above and to be protected against infringement.

For additional information about the Linköping University Electronic Press and its procedures for publication and for assurance of document integrity, please refer to its WWW home page: <http://www.ep.liu.se/>